

EXPERIMENTAL INVESTIGATION OF POTTING COMPOUND STRENGTH
ENHANCEMENT THROUGH THE USE OF CARBON NANOMATERIALS

A Thesis by

Jonathan Baalman

Bachelor of Science, Wichita State University, 2005

Submitted to the Department of Mechanical Engineering
and the faculty of the Graduate School of
Wichita State University
in partial fulfillment of
the requirements for the degree of
Master of Science

May 2008

© Copyright 2008 by Jonathan Baalman

All Right Reserved

EXPERIMENTAL INVESTIGATION OF POTTING COMPOUND STRENGTH ENHANCEMENT THROUGH THE USE OF CARBON NANOMATERIALS

The following faculty members have examined the final copy of this thesis for form and content, and recommend that it be accepted in partial fulfillment of the requirement for the degree of Master of Science with a major in Mechanical Engineering.

Bob Minaie, Committee Chair

Hamid Lankarani, Committee Member

Walter J. Horn, Committee Member

ABSTRACT

Carbon nanomaterials have recently been discovered which possess many unique physical properties. Multiple attempts have been made to integrate these materials into new technologies, including carbon nanocomposites with the goal of vastly improving the performance of these products. This thesis focuses on the incorporation of carbon nanofibers (CNF), multi-walled carbon nanotubes (MWNT), and buckminsterfullerenes (buckyballs) into Cytec's Corfil 625-1, an existing one-part potting compound. The goal was to improve the compressive strength of the material while maintaining the lap shear strength and keeping the density under that of a commercially available two-part potting compound, 3M's EC-3500.

The use of surfactants from BYK-Chemie led to an improvement in compressive strength of 45% when 5 wt% CNF was added. Carboxylic acid functionalization also showed improvement, however, CNF could not be added at a wt% as high as with the surfactant and a compressive strength enhancement of 11.5% was obtained. It was determined from SEM micrographs that preliminary mixing methods were breaking the glass balloons that were present in the 625-1 as provided by Cytec. As a result, the material was obtained without the microballoons and curing agent and new mixing methods were developed. The new compound allowed for greater flexibility in the mixing process, including higher shear and heating. It was also necessary to investigate the use of glass microballoons in order to replace what was not provided by Cytec. The use of S15 glass microballoons from 3M allowed for production of a potting compound similar to that of the 625-1 originally provided by Cytec. S38HS microballoons produced a one-part compound that was similar to the goal compound EC-3500. Sonication for 5 hours produced better results than the hand mixing that was initially performed, increasing the compressive strength of the potting compound by 21.7% when 1 wt%

functionalized CNF was added to the compound. MWNT of various sizes were investigated, with the smallest diameter nanotube (8 nm) providing the best improvement. A three roll mill was utilized as a new mixing method that would reduce complications and allow for the process to be scaled up producing larger batches of carbon nanocomposite. The number of times the material was run through the mill was an important parameter and a 30.9% improvement was acquired when the composite went through 7 times.

TABLE OF CONTENTS

Chapter	Page
1. INTRODUCTION	1
1.1 Carbon Nanomaterials.....	2
1.1.1. Buckminsterfullerenes	3
1.1.2. Carbon Nanotubes.....	6
1.1.2.1. General	6
1.1.2.2. Synthesis	8
1.1.2.3. Oriented Arrays.....	13
1.1.2.4. Growth Mechanisms	15
1.1.3. Properties of Carbon Nanotubes	16
1.1.3.1. Electrical Properties.....	16
1.1.3.2. Mechanical Properties.....	19
1.1.3.3. Thermal Properties.....	22
1.1.4. Applications of Nanotubes.....	23
1.1.5. Health issues	27
1.1.6. Summary.....	28
2. POTTING COMPOUND IMPROVEMENT	30
2.1 Introduction.....	30
2.2. Experimental	32
2.2.1. Materials Used	32
2.2.2. Dispersion Methods	35
2.2.3. Test Methods.....	39
3. RESULTS AND DISCUSSION.....	42
3.1. SEM of Nanofibers and Glass Microballoons	42
3.2. Functionalization and Surfactants	43
3.3. Hot Wet Testing.....	46
3.4. Investigation of New Glass Microballoons.....	47
3.5. Investigation of Ceramic Microspheres	49
3.6. Application of Vacuum to Samples	51
3.7. New Processing Methods.....	53
3.8. Amine Functionalization.....	55
3.9. Use of MWNT	57
3.10. EXAKT Three Roll Mill.....	59
4. CONCLUSIONS.....	62
REFERENCES	65

LIST OF TABLES

Table	Page
1. Mechanical properties of Corfil 625-1.....	33
2. Properties of glass microballoons	34
3. Properties of ceramic microspheres	34
4. Summary of composites used	40

LIST OF FIGURES

Figure	Page
1. Schematic of the pulsed supersonic nozzle used to generate fullerenes [1].	4
2. (a) The icosahedral C ₆₀ molecule. (b) The C ₇₀ molecule as a rugby ball-shaped molecule. (c) The C ₈₀ molecule as an extended rugby ball-shaped molecule. (d) The C ₈₀ molecule as an icosahedron [10].	5
3. The chiral vector \overrightarrow{OA} or $\overrightarrow{C_h} = n\hat{a}_1 + m\hat{a}_2$ is defined on the honeycomb lattice of carbon atoms by unit vectors \hat{a}_1 and \hat{a}_2 and the chiral angle θ with respect to the zigzag axis [10].	6
4. Molecular models of SWNT exhibiting different chiralities: (a) armchair configuration, (b) zig-zag arrangement, and (c) chiral conformation [11].	7
5. Cathode deposit obtained after arcing two graphite electrodes in a He atmosphere: (a) cross section of the deposit showing black inner core and a hard outer shell in gray; (b) side view of the same deposit showing only the gray, hard outer shell [11].	9
6. Experimental setup for the production of SWNT and MWNT using the laser technique. A high-power laser is focused on a composite graphite target inside a furnace at 1200C in an Ar atmosphere [11].	10
7. Apparatus used in Pyrolytic Carbon Nanotube production [20].	11
8. Schematic of a PECVD set-up [21].	12
9. Schematic of the electrolysis set-up used to produce CNT in the liquid phase [22].	13
10. (A) SEM micrograph of carbon nanotubes. (B) Enlarged view of (A) showing the diameters and their distributions. A site density of about 10^7 tubes/mm ² was estimated [25].	14
11. (a) An SEM micrograph and (b) a schematic showing the straight/curled nanotube structure produced by an alternating plasma and thermal process indicating both the field induced alignment effect and the base growth mechanism. (c) TEM micrograph showing a bundle of nanotubes [26].	14
12. Growth mechanism postulated by Baker for the formation of carbon filaments by pyrolysis of acetylene (C_2H_2) on a metal particle (M); (C) denotes carbon [11].	15
13. Schematic illustration of the growth mechanism proposed for carbon fibers and filaments from benzene pyrolysis over catalytic particles [11].	15

LIST OF FIGURES (continued)

Figure	Page
14. Representation proposed for carbon filament growth from Fe-Pt/C ₂ H ₂ systems (86). Carbon also diffuses through the metal, but the particle always remains at the bottom of the filament [11].	16
15. Chiral vectors for metallic and semiconducting nanotubes [10].	17
16. STM image (a) along with molecular model (b) used to determine chiral vector of nanotube [33].	17
17. Examples of electrodes to measure electrical properties of carbon nanotubes (a) 1.4 nm SWNT deposited on nanofabricated platinum electrodes (b) MWNT connected to four tungsten wires (80nm) [11].	18
18. Young's modulus for nanotubes measured by vibrations with TEM [35].	20
19. Arc-discharge nanotube exited by externally applied electric field at (a) off-resonance and (b) on-resonance [36].	20
20. Carbon nanotube in highly strained configuration (16%). (a) initial configuration, (b) bent upward, (c) bent back on itself, (d) bent in opposite direction. Size of nanotube: 850 nm long, 10.5 nm in diameter [38].	21
21. (a) HRTEM image of kink structure formed under mechanical stress in 1.2nm nanotube (b) Atomic structure obtained through computer simulation [39].	21
22. The thermal conductance of an individual 14 nm MWNT. Lower inset: Solid line represents $k(T)$ of an individual MWNT, broken and dotted lines represent small (OD 80 nm) and large bundles (OD 200 nm) of MWNT, respectively. Upper Inset shows the SEM image of device used for measurements [41].	23
23. (a) Cross-section of a fluorescent display with a field emission cathode constructed from MWNT; (b) picture of a bluelighting element [45].	24
24. Sketch of TV display utilizing carbon nanotubes [45].	25
25. (a) and (b) SEM images of AFM tip with attached MWNT, (c) TEM image showing MWNT structure [46].	26
26. SEM images showing process of cutting a nanotube with the nanoknife [47].	27

LIST OF FIGURES (continued)

Figure	Page
27. (A) Assembled Composite Sandwich Structure, (B) Composite Facesheet, (C) Honeycomb Core.....	30
28. Sonicator used for processing.	35
29. Sonication process.....	36
30. Representation of carbon nanotube functionalized with carboxylic acid group	36
31. Raman Spectroscopy verification of carbonyl group.....	37
32. Schematic of amine functionalization procedures	39
33. Schematic of Three Roll Mill.....	41
34. SEM images of potting compound with CNF 1. 15,000X view of CNF in potting compound 2. 90,000X close up of CNF aggregate 3. 85X view of microballoons in potting compound 4. 1,100X close up of broken microballoons	43
35. Summary of results obtained for all modified compounds (a) density, (b) compression strength, (c) lap shear strength.....	44-45
36. Results of hot-wet testing (a) lap shear strength, (b) compressive strength	46-47
37. (a) Compression results for glass microballoons, (b) Lap Shear results for glass microballoons, (c) Density results for glass microballoons	48-49
38. (a) Compression results for Ceramic Microspheres, (b) Lap Shear results for Ceramic Microspheres, (c) Density results for Ceramic Microspheres.....	50-51
39. (a) Compression results for applying vacuum, (b) Lap Shear results for applying vacuum, (c) Density results for applying vacuum.....	52-53
40. (a) Compression results for new processing method, (b) Lap Shear results for new processing method, (c) Density results for new processing method, (d) Compression/Density results for new processing method.....	54-55
41. (a) Compression results for amine functionalization, (b) Lap Shear results for amine functionalization, (c) Density results for amine functionalization.....	56

LIST OF FIGURES (continued)

Figure	Page
42. (a) Compression results using MWNT, (b) Lap Shear results using MWNT, (c) Compression/Density results using MWNT, (d) results using MWNT, (e) Lap Shear/Density results using MWNT	57-59
43. (a) Compression results using three roll mill, (b) Lap Shear results using three roll mill, (c) Density results using three roll mill, (d) Compression/Density results using three roll mill, (e) Lap Shear/Density results using three roll mill.....	60-61

CHAPTER 1

INTRODUCTION

In the aircraft industry, potting compounds are used to reinforce honeycomb core in sandwich structure. Multiple compounds are used based on their strength and density. The stronger, denser materials are two-part compounds requiring an additional mixing process compared to the lower strength compounds generally available as one-part systems. This thesis investigates the potential of enhancing an existing one-part compound (Corfil 625-1) to obtain the mechanical properties of the EC-3500 two-part system. Carbon nanomaterials have recently been discovered which possess many unique physical properties. Carbon nanofibers (CNF), multi-walled carbon nanotubes (MWNT), and buckminsterfullerenes (buckyballs) are used as nano-sized fillers with the potential of increasing the compressive strength of Corfil 625-1 while keeping the low density and maintaining the lap shear strength. A review of the nanomaterials used in this work is provided in this chapter. The second chapter focuses on the materials and methods used to produce the nanocomposite, while the third chapter provides results obtained using these methods. The final chapter concludes the thesis with a summary of the work performed.

The work done in this thesis consists of mixing CNF into Corfil 625-1 as provided by Cytec using surfactants and carboxylic functionalization. Two surfactants were used (BYK Chemie 164 and 191) to disperse the CNF at various weight percentages. Carboxylic acid functionalization was performed and the resulting CNF was mixed at 1.5 and 3.0 wt%. A portion of these materials were then selected to be placed in a hot-wet chamber for environmental conditioning. The effect of moisture and heat was thus determined for the selected composites. SEM work was then performed to determine the level of dispersion obtained and observe any

other changes in the potting compound. After this, three types of glass microballoons and two types of ceramic microspheres were selected to be used in the potting compound provided by Cytec without their microballoons. Vacuum was applied to the samples to determine if any air was being added during the processing. Next, new mixing methods were developed involving homogenization and increased sonication times. An amine functionalization was attempted which could lead to covalent bonding with an epoxy group in the resin. MWNT were then obtained in three different sizes (8 nm, 20-30 nm, and 50 nm) to be mixed into the potting compound. Finally, a three roll mill was used to disperse the MWNT along with buckminsterfullerenes by passing the composite through the mill various numbers of times.

1.1 Carbon Nanomaterials

Two forms of purely covalently bonded carbon have recently been discovered; fullerenes and carbon nanotubes. Fullerenes are carbon molecules consisting of a closed spherical arrangement of carbon atoms attached by single and double bonds while carbon nanotubes have a tube-like arrangement and can be divided into Multi-Walled Nanotubes (MWNT) and Single-Walled Nanotubes (SWNT).

Carbon Fullerenes (popularly known as buckyballs) were discovered in 1985 by Kroto [1]. This group observed that 60 carbon atoms are arranged in a soccer ball shape with the carbon atoms placed at the vertices of the polyhedrons. In later research they found fullerenes with varying numbers of carbon atoms (30-350) in each molecule. Fullerenes were fabricated using laser-beam vaporization of high purity graphite and were first observed using high definition electron microscopy. The discovery of this nanostructure has led to multiple studies of the synthesis, structure, properties, growth mechanisms, and possible applications.

MWNT were discovered by Iijima in 1991 [13], although literature suggests that MWNT had already been observed in the mid 1970s [12] by Endo. These structures were first fabricated using an arc discharge method and consisted of several concentric helical shaped carbon tubes of different diameters in the nanoscale range. In 1993, Iijima reported observing single-shell carbon nanotubes with diameters as low as 2.2 nm [14]. Theoretical and experimental research characterized the nanotubes, finding that this structure had properties not seen in any other material. These findings led to an explosion in the carbon research community; new developments and applications related to carbon nanomaterials are now being published at a rate of thousands of papers per year.

The synthesis, structure and properties of these carbon nanomaterials will be discussed in this thesis. The synthesis includes the various methods along with the apparatuses used to produce carbon nanostructures. The structure and characterization of nanoparticles is summarized with an attempt to link the structure with key properties such as electrical, mechanical and thermal properties discussed in a later section. A review of possible applications for these nanomaterials is also covered to give a comprehensive view of the capabilities of these nanomaterials. Finally, the latest research on health risks related to fullerenes and carbon nanotubes has been summarized in this chapter.

1.1.1. Buckminsterfullerenes

A Buckminsterfullerene or C_{60} is a molecule comprised of 60 carbon atoms arranged at the vertices of a polygon shape with 32 faces (12 pentagons and 20 hexagons). The shape of this molecule is like a soccer ball. Kroto [1] proposed to name this type of molecule Buckminsterfullerene after the architect and inventor Buckminster Fuller [2] who designed structures that resembled the shape and arrangement of the carbon atoms in C_{60} . They were first

produced by pulsed laser vaporization of carbon atoms in a rotating graphite disk (Figure 1). After vaporization, the atoms were transported by a Helium flow in which they cool, react and cluster.

C_{60} have a molecular diameter of approximately 7 Å with an average C-C atom of 1.44 Å [3]. Each carbon atom has two single bonds (~1.46 Å) and one double bond (~1.40 Å) [5]. Double bonds can be found on an aromatic ring-like structure of the hexagons, while single bonds are found on the pentagon-like faces [5].

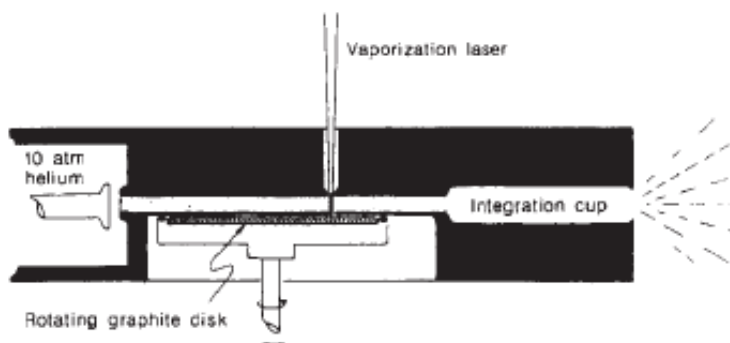


Figure 1. Schematic of the pulsed supersonic nozzle used to generate fullerenes [1].

There are other types of Fullerenes ranging from 30 to 350 carbons per molecule [1],[6],[7]. Diederich [6] separated and described other types of higher fullerenes that varied from C_{60} up to C_{250} . The extract usually contained approximately 65% of C_{60} , 30% of C_{70} , and 5% of higher fullerenes (mainly C_{76} , and two isomers of C_{78}). Figure 2 shows the most common types of fullerenes [5].

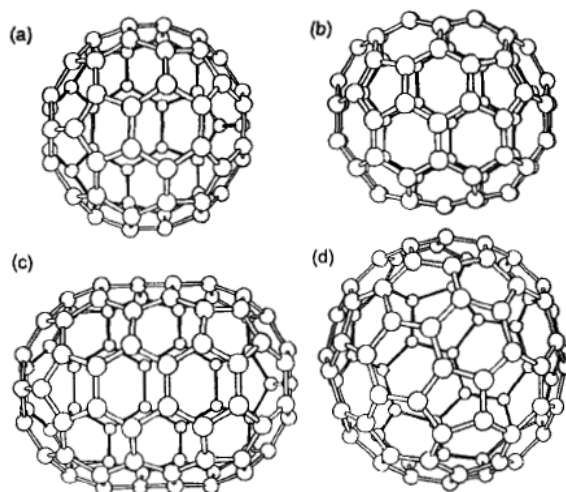


Figure 2. (a) The icosahedral C₆₀ molecule. (b) The C₇₀ molecule as a rugby ball-shaped molecule. (c) The C₈₀, molecule as an extended rugby ball-shaped molecule. (d) The C₈₀ molecule as an icosahedron [10].

Fullerenes were first synthesized by the laser evaporation of carbon sheets [1], and in 1990 Krätschmer [8] reported another process to fabricate high amounts of fullerenes by evaporating graphite electrodes in an atmosphere of ~100 torr of helium. In this process, the initial material was pure graphitic carbon with a low percentage of C₆₀. The black soot produced was then scraped from the walls of the reactor and dispersed in benzene. The benzene was then removed by heating to leave only the crystalline carbon material. The compound was then analyzed using mass spectrometry. Peaks were found for C₅₂, C₅₄, C₅₆, C₅₈, C₆₀, and C₇₀ with higher quantities of C₆₀ and C₇₀.

There has been no conclusive growth mechanism proposed; however, Smalley [7] suggested a growth path for fullerenes in which they follow the "pentagon road." He suggests that "the most favored form of any open graphitic sheet is the one which (a) is made up of only pentagons and hexagons, (b) has as many pentagons as possible, while (c) avoiding adjacent pentagons." This has been an extensive area of research due to the unique properties of the

fullerenes, their possible applications and the need to understand process parameters in the making of fullerenes. At room temperature C_{60} crystallizes in a face-centered cubic structure [3] with the lattice constant about 14.17 Å and the distance between C_{60} molecules about 10.02 Å [9]. The crystal structure of fullerenes is important in understanding its properties that will be discussed in the next section.

1.1.2. Carbon Nanotubes

1.1.2.1. General

Carbon nanotubes are a relatively new "man-made" material composed of pure carbon that can be visualized as a hexagonal graphene sheet rolled over and capped by half a C_{60} molecule on both ends of the tube. There are two different types of carbon nanotubes: single-walled nanotubes (SWNT) and multi-walled nanotubes (MWNT). A SWNT can be better visualized by referring to Figure 3 [10]. In a graphene sheet, the vector \overrightarrow{OA} is placed parallel to the graphene lattice constant. The points O and A are connected with vector $\vec{C}_h = n\hat{a}_1 + m\hat{a}_2$ where vectors \hat{a}_1 and \hat{a}_2 are unit vectors defined on the carbon structure. From points O and A , normals of \vec{C}_h can be drawn to obtain \overrightarrow{OB} and $\overrightarrow{AB'}$. If we take \overrightarrow{OB} and wrap it around to touch $\overrightarrow{AB'}$ we obtain a SWNT defined by n and m .

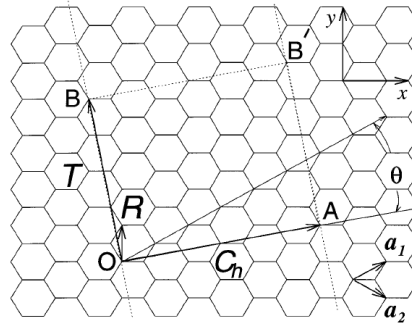


Figure 3. The chiral vector \overrightarrow{OA} or $\vec{C}_h = n\hat{a}_1 + m\hat{a}_2$ is defined on the honeycomb lattice of carbon atoms by unit vectors \hat{a}_1 and \hat{a}_2 and the chiral angle θ with respect to the zigzag axis [10].

Experimentally SWNT are defined by their diameter d_t and the chiral angle q using the following formulas [10]:

$$d_t = \frac{C_h}{p} = \frac{\sqrt{3}a_{c-c}(m^2 + nm + n^2)^{1/2}}{p}$$

$$q = \tan^{-1}\left(\frac{\sqrt{3}m}{m + 2n}\right)$$

where C_h is the length of the chiral vector \vec{C}_h and a_{c-c} is the nearest neighbor C-C distance. According to experimental work, three types of SWNT can be found, armchair (n,n), zig-zag ($q = 0^\circ$), and chiral (n,m). A schematic model of these types of SWNT can be seen in Figure 4 [11]. Further detail of the properties of these three types of CNT will be discussed later.

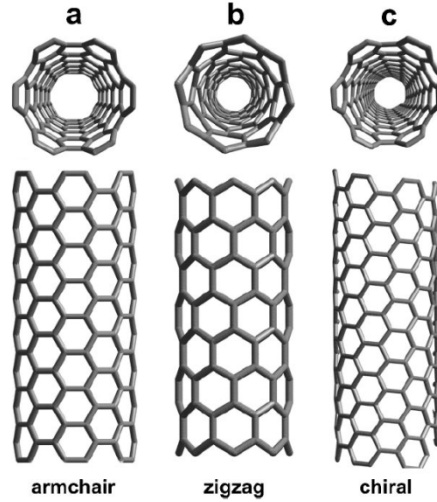


Figure 4. Molecular models of SWNT exhibiting different chiralities: (a) armchair configuration, (b) zig-zag arrangement, and (c) chiral conformation [11].

It has been reported in the literature [11], that images of MWNT were previously viewed by Endo in the mid 1970s when observing the internal structure of carbon fibers produced by pyrolysis [12], however at that time the research community was more interested in micrometer carbon fibers than in nanometer carbon tubes. MWNT were first reported by Iijima in 1991 when

he observed the main characteristics of the carbon compounds produced by arc discharge [13]. Iijima reported seeing microtubules of graphitic carbon consisting of "needle-like" tubes. He reported that each needle consisted of coaxial tubes of graphitic sheets that ranged from 2 to about 50 walls. The diameter of the smallest tubule found was $\sim 2.2\text{nm}$ and the average interlayer spacing was 3.4 \AA . The typical size of MWNT is an outer diameter of 2-20nm, inner diameter of 1-3nm, and a length of 1-100 μm [5].

Synthesis of SWNT were reported in 1991 [13] and 1993 by Iijima [14] and Bethune [15]. Later work by Iijima reported seeing "single-shell" carbon nanotubes [14] grown in the gas phase while Bethune and coworkers reported that co-vaporizing carbon and cobalt in an arc generator leads to the formation of SWNT with diameters as small as 1.2nm.

1.1.2.2. Synthesis

There are several different techniques to produce carbon nanotubes; these techniques include electrical arc discharge [11],[14]-[16], laser-vaporization [17]-[19], pyrolysis [20], CVD on metal catalyst [11],[21],[22], and electrochemical methods [23].

The arc-discharge method involves the passage of direct current through two high purity carbon graphite electrodes separated by a distance of 1-2 mm in an inert atmosphere (usually helium) [11]. During the process, carbon deposits on the cathode while the anode is consumed. This deposit is comprised of an external gray shell containing graphene layers and an internal dark, soft soot containing MWNT (Figure 5). SWNT can also be produced using arc discharge if a metal catalyst is included in the process. Iijima [14] used Fe-graphite electrodes to produce SWNT while Bethune [15] used a Fe-Co-Ni-graphite mixture in He atmosphere. Several research groups have developed other processes in order to increase the yield of SWNT. They can be produced using Gd, Co-Pt, Co-Ru, Co, Ni-Y, Rh-Pt, and Co-Ni-Fe-Ce catalyst materials

[11]. The Ni-Y mixture is widely used to produce SWNT in high yields (90%) [16]. The downside of this method is the elevated cost of production due to the required high purity of the materials (graphite and inert gases), the form of by-products such as encapsulated metal particles, and the lack of control over the dimensions of the SWNT.

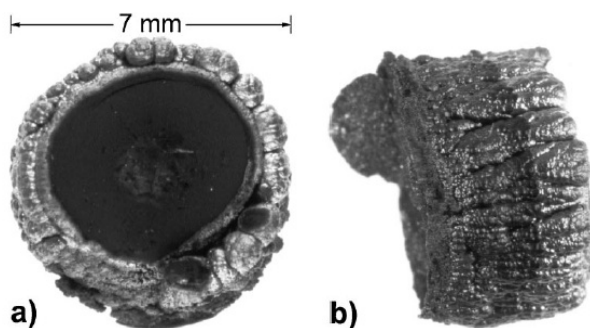


Figure 5. Cathode deposit obtained after arcing two graphite electrodes in a He atmosphere: (a) cross section of the deposit showing black inner core and a hard outer shell in gray; (b) side view of the same deposit showing only the gray, hard outer shell [11].

Laser-vaporization has also been used to produce carbon nanotubes [17]. It consists of a high power laser aimed at pure graphite targets capable of vaporizing carbon in a He atmosphere at 1200 °C. The idea behind this process is that the fullerene-type structure keeps one end open where other carbon particles attach to it, increasing the length of the tube. In order to produce SWNT, metallic particles have to be added to the carbon sheet. In 1996, Thess [18] used the laser-vaporization technique of C-Ni-Co mixtures at 1200 °C yielding more than 70% of SWNT which self-organized in ropes containing 100 to 500 SWNT. This procedure favored the metallic (10, 10) tube with open edge stabilized by triple bonds. Figure 6 shows the experimental setup for laser-vaporization.

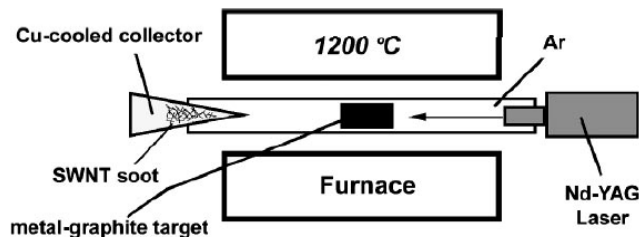


Figure 6. Experimental setup for the production of SWNT and MWNT using the laser technique. A high-power laser is focused on a composite graphite target inside a furnace at 1200C in an Ar atmosphere [11].

SWNT have also been produced using a CO₂-laser focused on graphite-metal targets where the oven can be eliminated if the inert atmosphere is substituted by Ar and N₂ [11]. In 2002 Eklund [19] reported producing high yields of SWNT (~1.5gr/h) using fast pulses from a free electron laser. The authors reported using only 20% of the average power of the 1kW Jefferson Lab free electron laser.

Pyrolytic growth of carbon nanotubes is also possible using pyrolysis. The same apparatus used to produce vapor grown carbon fibers (VGCF) was used with the partial pressure of the benzene much lower than what is usually used for VGCF [20]. The apparatus is shown in Figure 7. The procedure keeps benzene and hydrogen at 1000 °C for 1 hour of decomposition then the gas is cooled and the hydrogen is replaced by argon. The product is then collected from the substrate and analyzed using electron microscopy. The results show that pyrolytically grown SWNT are similar to those produced by arc discharge.

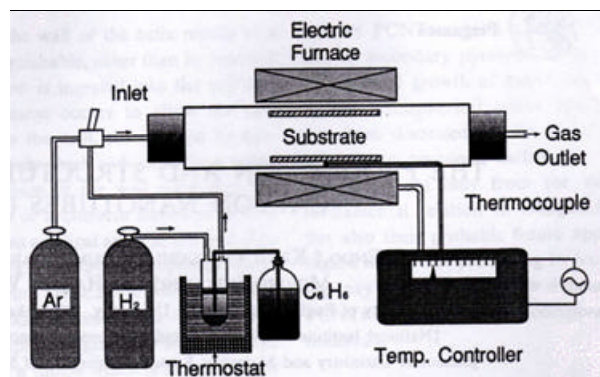


Figure 7. Apparatus used in Pyrolytic Carbon Nanotube production [20].

Chemical Vapor Deposition (CVD) using metal catalysts has been reported to be one of the most prominent methods of producing MWNT due to the ability to control many parameters of the process and produce different types of MWNT. There are many groups that describe different CVD methods to produce MWNT, a comprehensive review can be found in [11],[21],[22]. In this process, a metal coated substrate is used to attract the highly energized carbon. Once the carbon particles attach to the metal particles, they diffuse through and attach to other carbon particles which are also in highly energetic states producing long carbon fibers. The metal catalyst is extremely important since it determines the type of carbon nanoparticle produced. The different mechanisms proposed for the growth of MWNT using CVD can be found in [11]. Figure 8 shows details of the setup used in CVD.

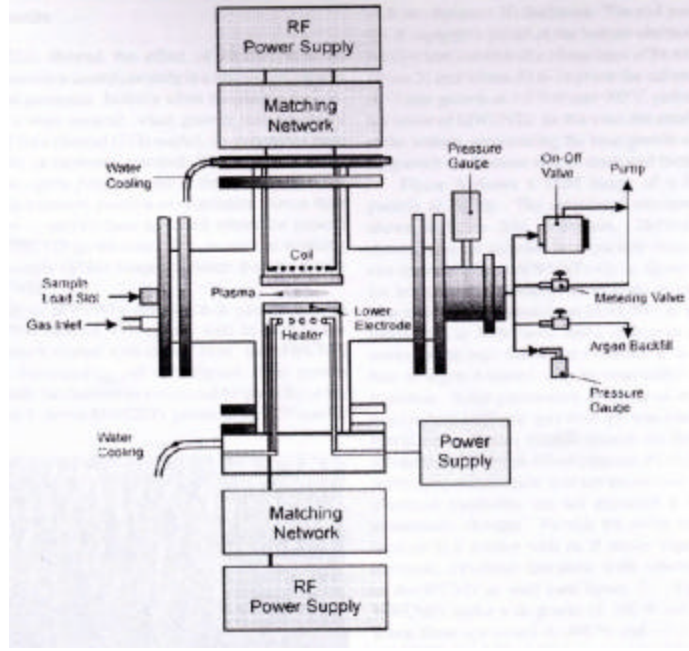
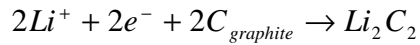


Figure 8. Schematic of a PECVD set-up [21].

A new electrochemical method for the growth of MWNT was proposed by Hsu. [23]. In this method, graphite electrodes are immersed in LiCl in an Ar atmosphere and DC voltage is applied between the electrodes. When the DC voltage is applied, the carbon dissolves in the molten salt producing Li_2C_2 . Then, C atoms segregate as an ordered hexagonal array, thus resulting in graphitic nanotubes. Figure 9 shows a schematic of this process. The following chemical formula was proposed for this reaction:



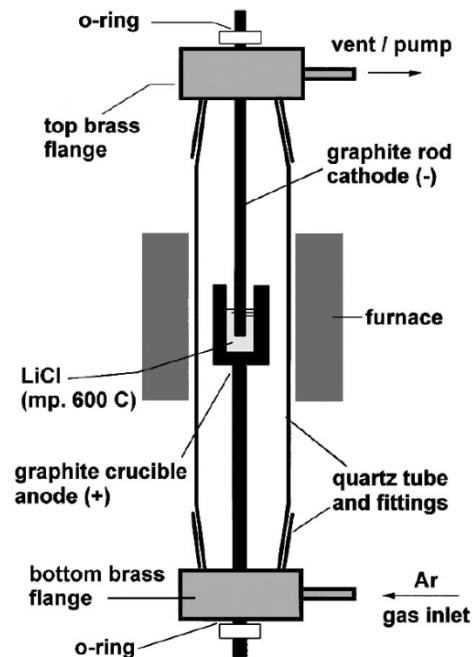


Figure 9. Schematic of the electrolysis set-up used to produce CNT in the liquid phase [22].

1.1.2.3. Oriented Arrays

CNT have also been grown in an orderly fashion using different CVD on metal catalysis techniques. In 1996, Li [24] was able to produce aligned MWNT by using a method based on CVD catalyzed by iron nanoparticles embedded in silica. The resulting nanotubes were spaced at about 100 nm with a length of 50 micrometers and a growth direction controlled by the pores of the silica substrate. Later work by Ren [25] achieved the synthesis of aligned carbon nanotubes on glass substrates coated with nickel at temperatures below 666 °C by using plasma-enhanced hot filament chemical vapor deposition. Resulting nanotubes had controllable dimensions with diameters from 20 to 400 nm and lengths from 0.1 to 50 micrometers. They attributed the alignment of the CNT to a "nanotube nucleation process catalyzed by ammonia and nickel. In the presence of ammonia each nickel cap efficiently catalyzes the continuous synthesis of carbon nanotubes." Figure 10 shows the MWNT grown using the latter method.

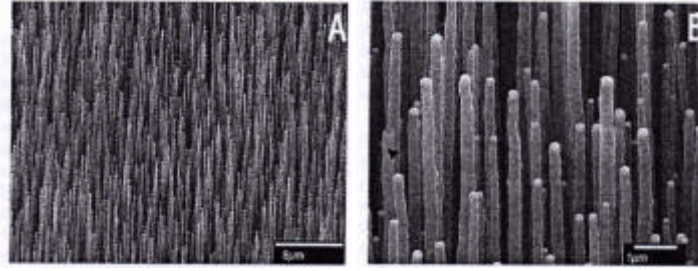


Figure 10. (A) SEM micrograph of carbon nanotubes. (B) Enlarged view of (A) showing the diameters and their distributions. A site density of about 10^7 tubes/mm² was estimated [25].

Further work by Bower [26] used plasma-induced alignment to fabricate carbon nanotubes. The authors suggested that the alignment is primarily induced by "the electrical self-bias field imposed on the substrate surface from the plasma environment." Figure 11 shows the nanotubes fabricated by Bower. Another important feature of this method was the high rate of growth (~ 100 nm/s) which can be used to produce MWNT on a commercial scale.

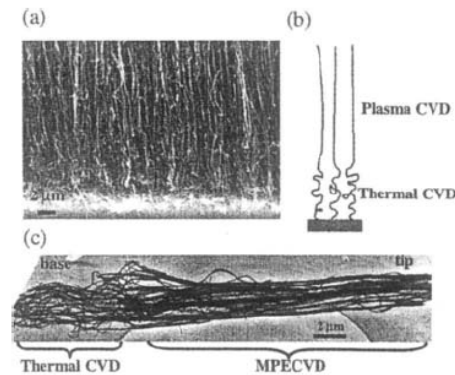


Figure 11. (a) An SEM micrograph and (b) a schematic showing the straight/curled nanotube structure produced by an alternating plasma and thermal process indicating both the field induced alignment effect and the base growth mechanism. (c) TEM micrograph showing a bundle of nanotubes [26].

1.1.2.4. Growth Mechanisms

According to Terrones [11], there are three accepted growth mechanisms for the fabrication of CNT. Figure 12, Figure 13 and Figure 14 show schematics of these three mechanisms. Figure 12 shows the first mechanism proposed by Baker [27]. Baker and coworkers proposed that filament growth occurs when the carbon that decomposes from acetylene diffuses through the metal particle and precipitates on the other side of the filament where the temperature is lower. The process continues until the carbon species stops reacting with the end particle or the catalytic activity ends.

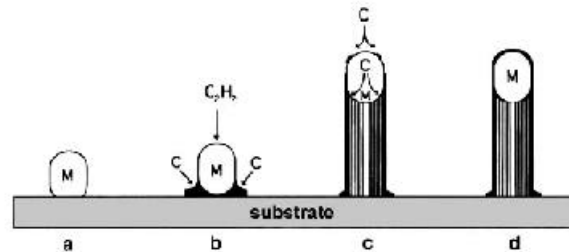


Figure 12. Growth mechanism postulated by Baker for the formation of carbon filaments by pyrolysis of acetylene (C_2H_2) on a metal particle (M); (C) denotes carbon [11].

The second growth mechanism proposed is depicted in Figure 13. This mechanism was proposed by Baird in 1974 [28] and Oberlin [12] in 1976 [11]. In this mechanism, the carbon diffuses on the surface of the metal particle, precipitating on the other end of the particle, thus forming the SWNT.

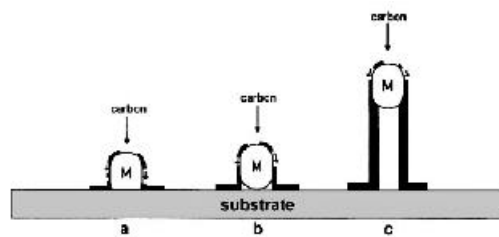


Figure 13. Schematic illustration of the growth mechanism proposed for carbon fibers and filaments from benzene pyrolysis over catalytic particles [11].

The third type of growth mechanism is depicted in Figure 14. In this mechanism the carbon filaments grow from their bases rather than their tips [29],[30], the carbon also diffuses through the metal, but the metal particle always remains at the base. This growth type was observed in pyrolysis experiments of acetylene over Fe-Pt substrates.

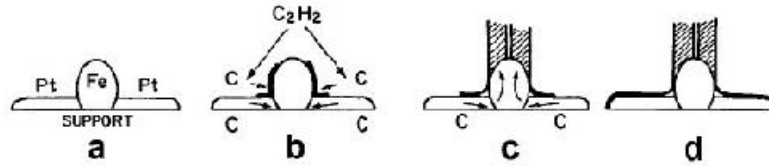


Figure 14. Representation proposed for carbon filament growth from Fe-Pt/C₂H₂ systems (86). Carbon also diffuses through the metal, but the particle always remains at the bottom of the filament [11].

1.1.3. Properties of Carbon Nanotubes

1.1.3.1. Electrical Properties

One of the most interesting properties of carbon nanotubes is the dependence of electrical conductivity on the geometry of the nanotube. A nanotube can be metallic or semi-conducting with varying energy gap depending on the chiral vector (n,m) that defines the tube. Two-dimensional graphite is a zero gap semiconductor with bonding and antibonding bands degenerate at the K-point of the hexagonal Brillouin Zone. If one of the few wave vectors that can propagate along the circumference passes through this K-point, metallic conditions result [31]. When a nanotube is in the armchair configuration (n,n), it is always metallic, if $n-m=3j$, where j is a non-zero integer, the nanotube is a very tiny gap semiconductor, and if $n-m=3j\pm1$, the nanotube is a large gap semiconductor. It has been determined that as the diameter increases, the band gaps of the large and tiny gap semiconductors decrease by $1/d$ and $1/d^2$, respectively. The tiny gap semiconducting nanotubes can therefore be labeled as metallic because the thermal

energy at room temperature is large enough to excite the electrons to the conducting bands [32].

Figure 15 shows metallic and semi-conducting nanotubes based on their chiral vectors [10].

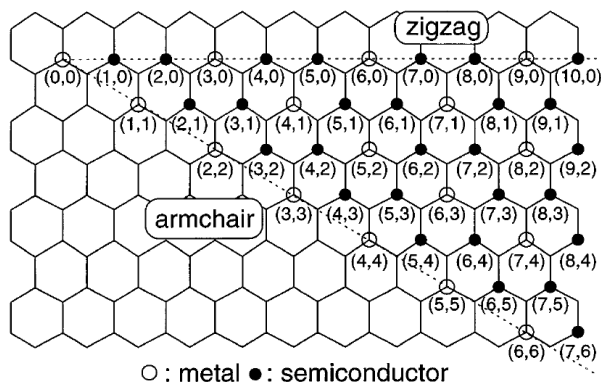


Figure 15. Chiral vectors for metallic and semiconducting nanotubes [10].

Analysis of carbon nanotubes by scanning tunneling microscopy (STM) can be performed to determine the diameter and orientation of the carbon rings which is used in defining the chiral vector (Figure 16). Scanning tunneling spectroscopy can then be used to determine the electrical properties of the nanotube and compare the results with those predicted by this model. Experiments have shown good agreement, those predicted to be metallic are indeed metallic [33].

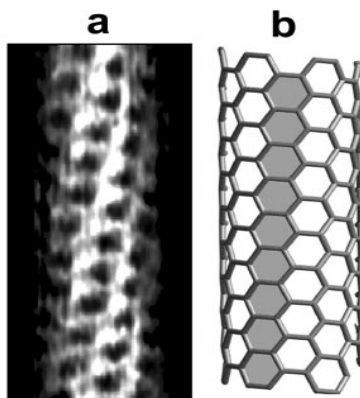


Figure 16. STM image (a) along with molecular model (b) used to determine chiral vector of nanotube [33].

A method used to measure the resistance of carbon nanotubes has been developed in which dilute suspensions of nanotubes are dispersed over patterned electrical contacts to connect two adjacent electrodes with a single nanotube.

Figure 17 shows an example of a SWNT connecting platinum and tungsten electrodes [11]. Theoretical calculations, based on p-electron transport, of the low-bias resistance of SWNT give a value of $h/4e^2$ or about 6 k Ω . Measurements using the above mentioned method give values closer to 1 M Ω . Reasons for the large difference include contact resistance between the nanotube and the metal electrode, re-hybridization of carbon bonds from sp² to sp³ at the interface and adsorbed species on the nanotube [34]. This difference in resistivity based on the presence of different chemical species could allow for the use of SWNT as very sensitive chemical sensors.

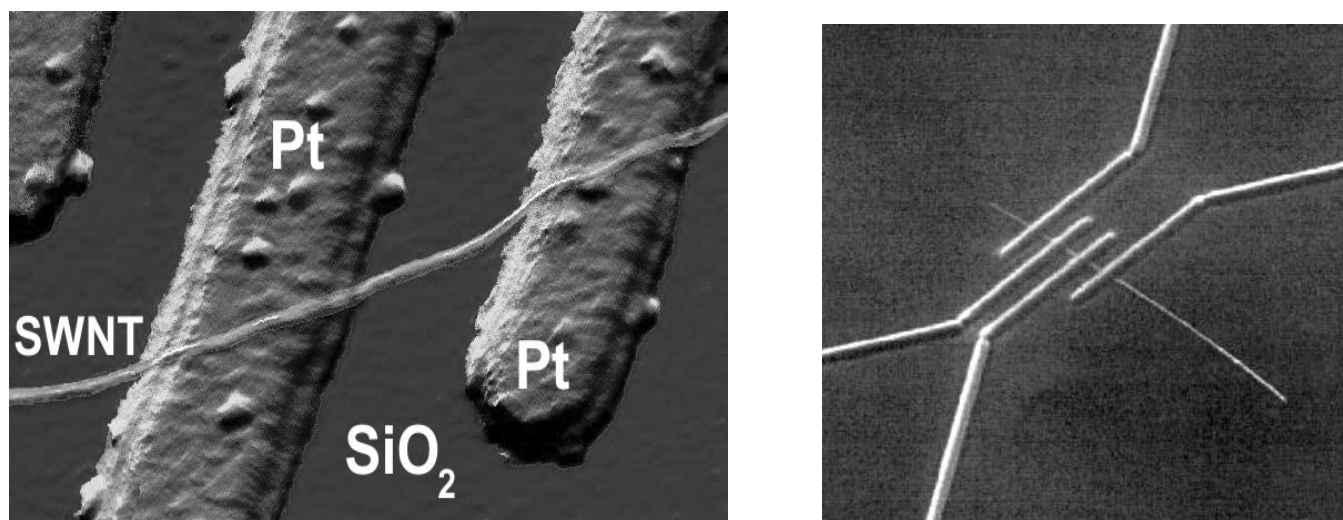


Figure 17. Examples of electrodes to measure electrical properties of carbon nanotubes (a) 1.4 nm SWNT deposited on nanofabricated platinum electrodes (b) MWNT connected to four tungsten wires (80nm) [11].

1.1.3.2. Mechanical Properties

Since carbon nanotubes were discovered, it has been expected that they would exhibit mechanical properties superior to those of any other known material. The carbon-carbon bond found in a grapheme layer is one of the strongest bonds found in nature and the nanoscale allows production with very few defects. Both of these factors lead to the conclusion of excellent mechanical properties. Accurately manipulating and measuring the properties of nanotubes is extremely challenging; however, methods have been developed and several research groups have reported values for the Young's modulus of carbon nanotubes. There are two primary methods for determining the Young's modulus. The first method used involves measuring the amplitude and frequency of oscillation of a nanotube fixed at one end by TEM and correlating this to the modulus, while the second measures the applied force as a function of displacement using an AFM. Terrones [11] summarizes results obtained from a variety of groups. The earliest measurement of the nanotube modulus was done in 1996 by Treacy [35]. Nanotubes produced by the arc discharge method were used in this study. The nanotube was assumed to be a clamped homogeneous cylindrical cantilever of length L , with outer and inner radii a and b , respectively. The given relation between undamped vibration frequency, ω_n , and Young's modulus, E , is

given as $\omega_n = \frac{b_n^2}{2L^2} \sqrt{\frac{E(a^2 + b^2)}{\rho}}$. Where ρ is the density of the nanotube wall, β is a constant, and

n is the vibrational mode. Using this equation, an average value of 1.8 TPa was found for the Young's modulus. A deviation of one order of magnitude was obtained, illustrating the experimental uncertainties and also variations from perfect nanotube structure. The results obtained are given in Figure 18. It should be noted that nanotubes with smaller diameters generally gave higher values for the modulus.

Nanotube no.	Length (μm)	Outer diameter (nm)	Inner diameter (nm)	Young's modulus (TPa)
1	1.17	5.6	2.3	1.06
2	3.11	7.3	2.0	0.91
3	5.81	24.8	6.6	0.59
4	2.65	11.9	2.0	1.06
5	1.73	7.0	2.3	2.58
6	1.53	6.6	2.3	3.11
7	2.04	7.0	3.0	1.91
8	1.43	6.6	3.3	4.15
9	0.66	7.0	3.3	0.42
10	1.32	9.9	3.0	0.40
11	5.10	8.4	1.0	3.70

Average value of Young's modulus is 1.8 TPa.

Figure 18. Young's modulus for nanotubes measured by vibrations with TEM [36]

Wang performed a similar study [36] using nanotubes produced by pyrolysis along with those produced by arc discharge. An example of the TEM images obtained is given in Figure 19. A decrease in modulus as the nanotube diameter increases was also observed; however, the highest value obtained with the arc discharge fibers was 1.2 TPa, lower than the average obtained by Treacy. Values for the nanotubes obtained by pyrolysis were almost 15 times lower than those made by arc discharge, with an average of 28 GPa. This is attributed to the high number of point and volume defects present in fibers fabricated by pyrolysis.

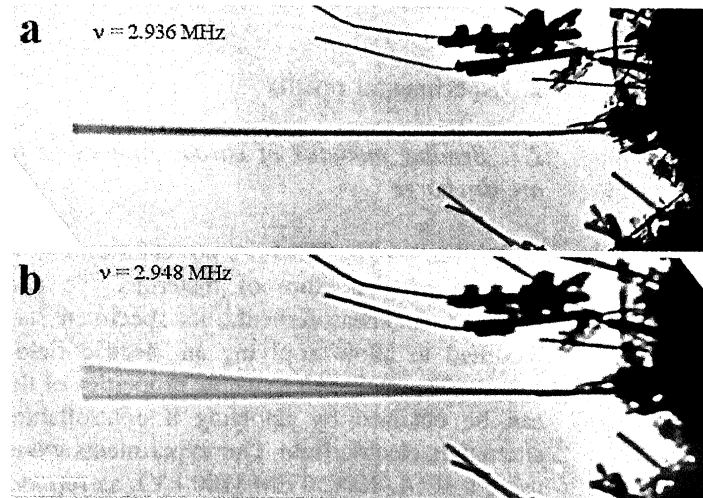


Figure 19. Arc-discharge nanotube excited by externally applied electric field at (a) off-resonance and (b) on-resonance [36].

Yu performed direct measurement of the carbon nanotube modulus using an AFM in 2000 and obtained values ranging from 0.32-1.47 TPa [37]. Falvo [38] used an AFM tip to repeatedly bend a MWNT through large angles without fracture showing that nanotubes are remarkably flexible and resilient. Figure 20 shows the bending of the nanotube from this study. Reversible, periodic buckling of the nanotube was observed along with up to 16% strain without separating the nanotube.

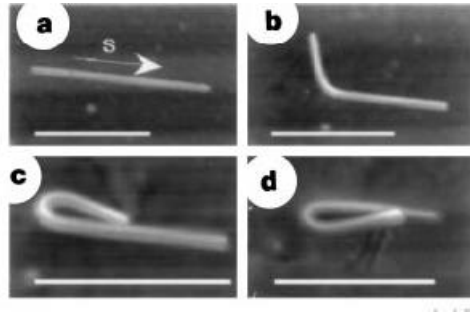


Figure 20. Carbon nanotube in highly strained configuration (16%). (a) initial configuration, (b) bent upward, (c) bent back on itself, (d) bent in opposite direction. Size of nanotube: 850 nm long, 10.5 nm in diameter [38].

Molecular dynamics simulations have also been used to simulate the mechanical properties of nanotubes. An example is given in [39] where a TEM image of a bent SWNT is used to create a model and results show that high reversible deformations are possible. Figure 21 shows images from this work.

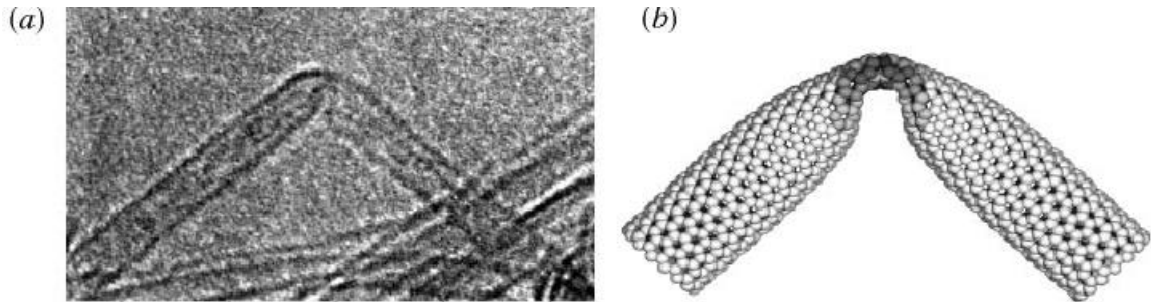


Figure 21. (a) HRTEM image of kink structure formed under mechanical stress in 1.2 nm nanotube (b) Atomic structure obtained through computer simulation [39].

A value for the breaking stress of nanotube ropes is given by Yu [37] as 55GPa, but values are expected to be much higher for a perfect nanotube. It is obvious that accurately measuring the properties of a single nanotube is a difficult process. There are many variables that contribute to the strength of a nanotube, including size and purity, both of which are affected by the method of fabrication. Initial measurements of the mechanical properties of nanotubes indicate that this is one of the strongest materials known to man and has great potential in many applications where high strength and low weight are needed.

1.1.3.3. Thermal Properties

The thermal properties of nanotubes have not been studied as extensively as the electrical and mechanical properties; however, it is believed that most of the thermal properties, including specific heat and thermal conductivity will resemble that of a two-dimensional graphene sheet. Yi performed thermal conductivity measurements on pyrolytically produced MWNT and observed that from 4 to 300 K there was a linear relationship between conductivity and temperature [40]. This same group also determined that the specific heat varies linearly with temperature from 10 to 300 K. Kim [41] showed that an individual nanotube displays a room temperature conductivity of 3000 W/K, similar to that of graphite and two orders of magnitude higher than bulk MWNT (Figure 22). It is presumed that smaller diameter nanotubes will exhibit conductivities much greater than graphite.

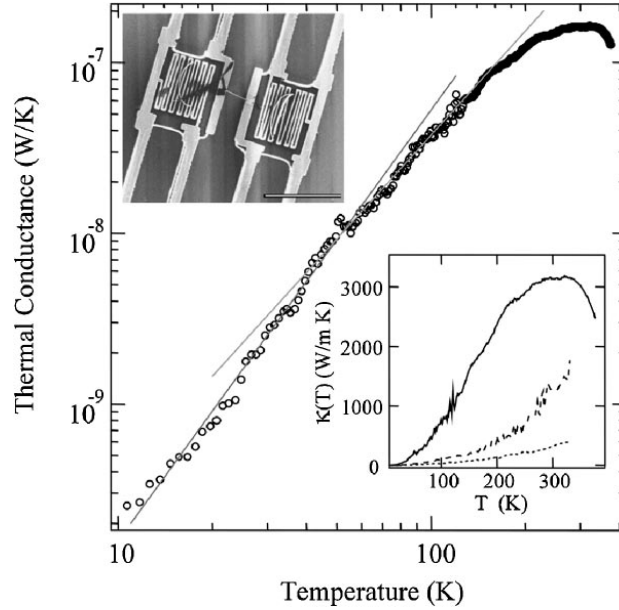


Figure 22. The thermal conductance of an individual 14 nm MWNT. Lower inset: Solid line represents $k(T)$ of an individual MWNT, broken and dotted lines represent small (OD 80 nm) and large bundles (OD 200 nm) of MWNT, respectively. Upper Inset shows the SEM image of device used for measurements [41].

Thermal expansion measurements have been performed by Maniwa [42] using an X-ray diffraction technique. The results are consistent with graphite. Almost no expansion exists along the nanotube axis ($-0.15 \pm 0.20 \times 10^{-15} / \text{K}$) but along the diameter direction a value of $0.75 \pm 0.25 \times 10^{-15} / \text{K}$ is observed between 300 and 950 K. This is still a very small value and can be attributed to the strong C-C bonds present in the nanotubes. It is expected that, just as with the electrical and mechanical properties, the thermal properties will change as the size of nanotube changes.

1.1.4. Applications of Nanotubes

Several possibilities exist for electronic devices made from nanotubes. A junction between a metallic nanotube and a semi-conducting nanotube has been proposed to act as a diode. A nanotube can be deposited on a surface to act as a gate, crossed nanotubes can act as rectifiers, and a crossed array can be used for random-access, non-volatile memory [43]. Another potential application which utilizes the electrical properties of carbon nanotubes is artificial

muscles. Sheets of SWNT could be used as electromechanical actuators to replace deteriorated muscle [44]. Field emission devices based on the fact that a carbon nanotube emits electrons from its tip when a potential is applied between it and an anode can be used as bright light sources or X-ray emitters (Figure 23). Very small field-effect transistor arrays have been fabricated showing the possibility of using SWNT in displays (Figure 24) replacing the current plasma and LCD versions [45]. The use of carbon nanotubes would enhance the brightness, viewing angle, operating temperature, response rate, and would consume less power than current displays. Logic circuit boards utilizing carbon nanotubes are also under development. As mentioned earlier, carbon nanotubes are also being investigated as potential sensors capable of signaling a very low concentration of a given airborne chemical. These sensors could be used to monitor leakage in chemical plants by detecting a pollutant concentration of less than 200 ppm. There are many difficulties that must be overcome in order to produce new reliable devices and to integrate the current designs into industrially feasible products.

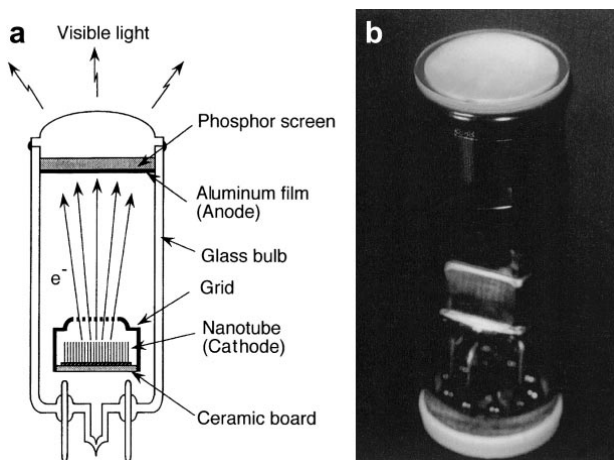


Figure 23. (a) Cross-section of a fluorescent display with a field emission cathode constructed from MWNT; (b) picture of a bluelighting element [45].

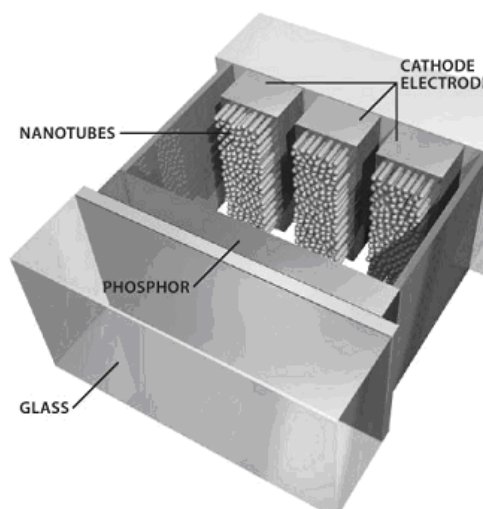


Figure 24. Sketch of TV display utilizing carbon nanotubes [45].

One of the most obvious and extensively studied applications for nanotubes is in the fabrication of polymer composites. The excellent electrical, mechanical, and thermal properties will allow for the production of multi-functional composite materials: composites that are not only stronger than traditional composites, but also have the ability to conduct electricity and heat. Many groups have attempted the manufacture of nanocomposites, but none have achieved the full potential of the carbon nanotube. Significant improvements have been made; including increases in elastic modulus, tensile strength, compressive strength, and toughness with as little as 1 wt% nanotube. The major difficulties in creating a nanocomposite are achieving a homogenous dispersion of individual nanotubes rather than the large bundles that typically occur and ensuring compatibility between the surface of the nanotube and the polymer so that stress can be transferred to the nanotube. Methods to overcome the dispersion problem include sonication and new methods of high shear mixing. Surfactants and chemical functionalization can be used to enhance the surface interactions and increase stress transfer. Nanotubes are also being added to ceramic and metal matrices to improve their properties.

Another current application of nanotubes is as scanning probe microscopy (SPM) tips [46]. The nanometer size increases resolution as compared to traditional tips. The strength of the nanotube also increases the lifetime of the scanning tip. Further modifications of the MWNT tip make it useful in other forms of SPM. Chemically functionalized tips can be used in chemical force microscopy and magnetic particles can be attached to the end of the nanotube to be used in magnetic force microscopes (Figure 25). The MWNT tip can also be used in nanofabrication and nanolithography in the form of “nano-tweezers” or as “nano-knives”. Figure 26 shows an example of a nanotube attached to a metal tip which is used to precisely cut and sharpen other nanotubes [47].

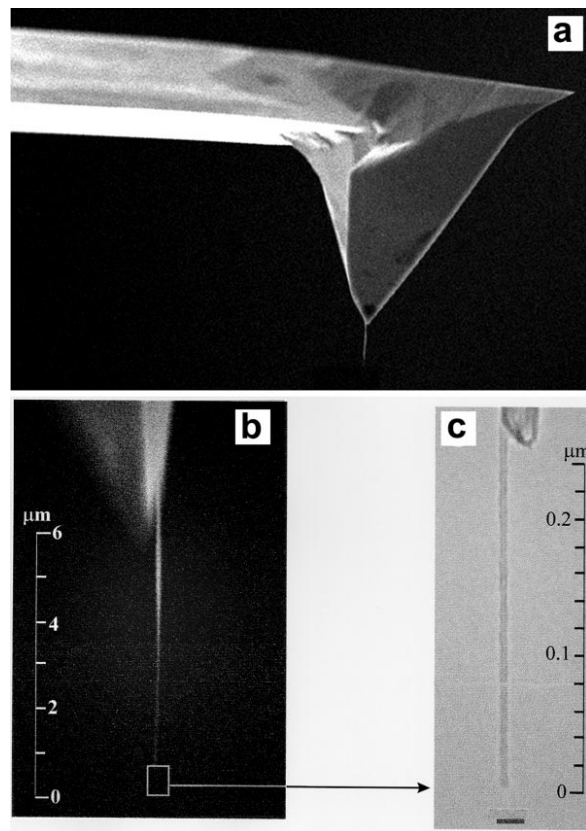


Figure 25. (a) and (b) SEM images of AFM tip with attached MWNT, (c) TEM image showing MWNT structure [46].

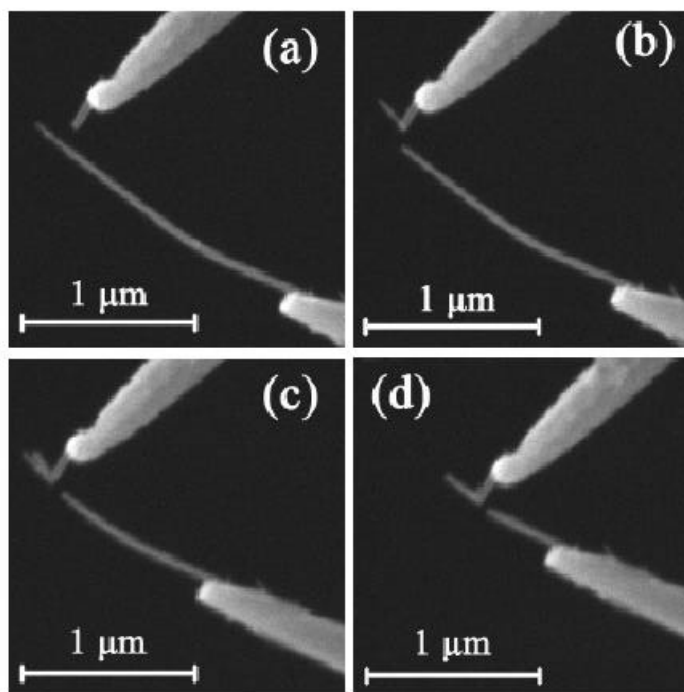


Figure 26. SEM images showing process of cutting a nanotube with the nano-knife [47].

1.1.5. Health issues

A small amount of research concerning the impact of carbon fullerenes on living species has been reported in the literature. However, research is inconclusive as some studies show no ill effects while other research indicates toxic effects of nanotubes even to the point of causing death. Continued research is needed to ensure that carbon nanoparticles are safe enough to be used in commercial products and to determine guidelines for use in a research environment.

On the one hand, research in 2006 [50] showed that pristine C_{60} not dissolved in water are non-toxic to cultured cells when treated with up to 200 $\mu\text{g/ml}$ (200 ppm). The authors determined that C_{60} are not toxic since they do not alter morphology, cytoskeletal organization, cell cycle dynamics, or inhibit cell proliferation. Huczko [51] carried out experiments dealing with skin allergies when exposed to fullerene soot. In this study, the author conveys that fullerene soot is unlikely to be associated with any risk of skin irritation and allergy. In 2001,

Huczo [57] reported that guinea pigs treated with CNT made by arc sublimation of graphite did not induce any abnormalities of pulmonary function or measurable inflammation. Other research by Yoko [49] showed that C₆₀ dissolved with poly(vinylpyrrolidone) in the presence of light, acted as an antibacterial agent, exposing the potential health benefits of fullerenes.

Carbon nanotubes can also be harmful as shown by Huczko [52]. The pulmonary toxicity of nanotubes in Guinea pigs was studied and the results showed that the duration of exposure and material characteristics can affect the respiratory process and induce pathological reaction in lung tissue. In 2006, Muller [53] found that if CNT reach the lungs they can exert serious toxicity as shown in experimental animals with inflammatory and fibrotic reactions. Further work [54] studied the in-vitro cytotoxicity of SWNT, MWNT, and fullerenes. The authors reported intense cytotoxicity of SWNT in alveolar macrophages after 6 h exposure. The ranking order of cytotoxicity on a mass basis was SWNT>MWNT>quartz>C₆₀. In terms of the toxicity of SWNT in skin cells, Shvedova [55] showed that immortalized human epidermal keratinocytes exposed to SWNT show oxidative stress and cellular toxicity by the creation of free radicals, accumulation of peroxidative products, antioxidant depletion, and loss of cell viability [56]. In 2006, Shigian [48] reported that water soluble fullerenes induced lipid peroxidation (LPO) in the brains of juvenile largemouth bass leading to death. A review on toxicological effects of carbon nanoparticles can be found in [53],[56],[57].

1.1.6. Summary

A review of the synthesis, characterization, properties, and applications of fullerenes and carbon nanotubes has been presented. The equipment and methods of fabricating fullerenes and CNT have been explored; these techniques include arc-discharge, laser-vaporization, pyrolysis, CVD on metal catalyst, and an electrochemical method. Also, the synthesis of oriented carbon

nanotubes on metal coated substrates was discussed. The three most accepted growth mechanisms of carbon nanostructures using CVD on metal catalyst were then described: diffusion of carbon particles through the metal catalyst at the tip of the CNT, diffusion of carbon particles on the surface of the catalyst at the tip of the CNT, and diffusion of carbon atoms on the metal catalyst at the base of the CNT.

The properties of the CNT were also discussed. Due to their unique mechanical, electrical and thermal properties, carbon nanotubes have been the focus of much recent research. Some applications of CNT were explored and described. The main applications include nanocomposites, electronic devices and microscopy tips. The health related issues concerning the manipulation of fullerenes and CNT were summarized to provide the reader some useful information on working with CNT.

CHAPTER 2

POTTING COMPOUND IMPROVEMENT

2.1 Introduction

Potting compounds are used in the aircraft industry to reinforce honeycomb core in sandwich structures, see Figure 27, most commonly around fastener locations. Desirable qualities for a potting compound include low density, high compressive and shear strength, flexibility in the uncured state to allow for working into the core, and compatibility with the cure cycle used for the sandwich structure. In addition, a one-part material is preferred over a two-part material due to manufacturing difficulties associated with two-part compounds.

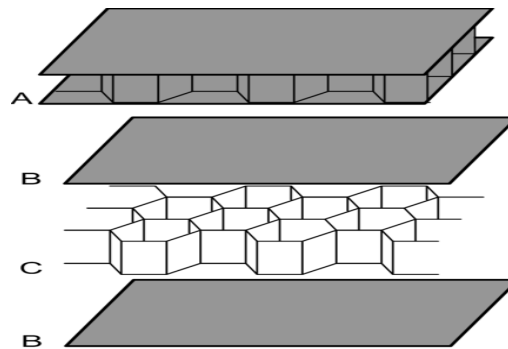


Figure 27. (A) Assembled Composite Sandwich Structure, (B) Composite Facesheet, (C) Honeycomb Core.

Commercially available materials generally provide trade-offs of these characteristics. For example, 3M's EC-3500 has high mechanical strength and acceptable density, but has the disadvantage of being a two-part epoxy. One-part potting compounds with mechanical properties similar to those of EC-3500 tend to be heavier (Cytec's Corfil 623-1), and those that are lighter do not have adequate strength (Cytec's Corfil 625-1).

The purpose of this work was to investigate modifications of a low density, one-part potting compound and identify those that would improve the compressive strength of the resulting compound to match that of EC-3500 (10,000 psi) and maintain the low density of Corfil 625-1 (26-32 lb/ft³). It was shown in the previous chapter that carbon nanomaterials exhibit extremely high elastic modulus and strength along with other desirable properties; therefore, they will be used as potential reinforcement.

Carbon nanofibers (CNF), multi-walled carbon nanotubes (MWNT), single-walled carbon nanotubes (SWNT), and buckyballs were added to Corfil 625-1 in an attempt to improve the compressive and shear strengths of the potting compound. The nanomaterials were added at different weight percentages to determine the amount that would result in the greatest enhancement of properties. As previously mentioned, the two main difficulties to overcome in the production of nanocomposites are the dispersion of the nanomaterial in the composite matrix and bonding of the nanomaterial with the matrix. If the nanoparticles are not uniformly dispersed, the full potential of the composite will not be reached. Poor dispersion results in clumps or aggregates of nanoparticles which negate the benefits of the very small size of an individual nanoparticle. This also leads to areas in the composite which have no nanomaterial reinforcement and are therefore weak areas in the composite. If there is not a favorable bonding between the nanomaterial and the composite matrix then no stress is transferred to the nanomaterial and it acts as a void or inclusion, reducing the strength rather than improving it.

Other materials used to modify the properties of the potting compound included glass microballoons and ceramic microspheres. These were added at much higher percentages than the carbon nanomaterials and are commonly available in the aircraft industry as strength/density

modifiers. The difficulties with dispersion and bonding associated with nanomaterials are not a factor when working with these glass and ceramic materials.

Several mixing methods were used to achieve the required level of dispersion and techniques were also employed to improve the bonding between the individual nanotubes and the potting compound. The potting compound/CNF composites were tested and compared with raw 625-1. The effect of moisture and temperature on the resulting composite material was also examined through hot/wet testing of the more promising mixtures.

2.2. Experimental

2.2.1. Materials Used

The potting compound used was Cytec's Corfil 625-1, which is a one-part toughened potting compound system formulated for use in insert and edge filling of honeycomb core. Corfil 625-1 can be cured at either 250°F or 350°F with minimal to no exotherm in large applications. It is formulated to have relatively low viscosity making it especially suitable for use with automated equipment. Although Corfil 625-1 is considered to be a one-part resin system, it contains glass microballoons that reduce the density. Table 1 contains the mechanical properties for Corfil 625-1 as provided by Cytec. The Corfil 625-1 base material without the microballoons and curing agent was also obtained. This allowed for more freedom in the processing of the nanocomposite. It was observed that the glass microballoons were being broken during mixing which resulted in undesirable properties (higher density and lower strength). By adding the microballoons after the nanomaterial was dispersed, higher shear loads could be applied during the mixing process without breaking any of the glass microballoons, resulting in a better dispersion. Having the curing agent separate from the main resin system was also helpful, allowing for heat to be applied to the resin system without initiating the curing of the potting

compound. This allowed for heating of the potting compound to remove any solvents used in the dispersion process.

TABLE 1
MECHANICAL PROPERTIES OF CORFIL 625-1

Density (lb/ft³)	25-31
Compression strength (psi)	3000
Lap shear strength (psi)	1200

Initial work was done to enhance the dispersion and bonding of CNF within the Corfil 625-1 as provided by Cytec. The carbon nanofibers used had diameters varying from 60 nm to 150 nm and lengths ranging between 30 μm and 100 μm . The tensile modulus and strength for these fibers were estimated by Applied Sciences: Pyrograf Products Inc. to be 600 GPa and 7 GPa respectively.

Since Corfil 625-1 did not contain the microballoons, the correct type and amount of glass microballoon that would lead to a compound comparable to stock Corfil 625-1 had to be determined. Several samples with different density and strength were obtained from the 3M Corporation. The material properties of these are provided in Table 2. Work was done to obtain a potting compound as close to the stock Corfil 625-1 as possible using the available microballoons and to investigate the potential of increasing the strength of the potting compound through the use of glass microballoons alone.

TABLE 2
PROPERTIES OF GLASS MICROBALLOONS

Microballoon	Density (lb/ft ³)	Crush Strength (psi)
S15	9.36	300
S38HS	23.72	5,500
S60HS	37.46	18,000

Ceramic microsphere filler was also obtained from the 3M Corporation. The material properties of these fillers are provided in Table 3. The ceramic fillers were chosen because of their high compressive strength, but they had the drawback of having higher densities. In order to obtain a low density potting compound, the glass fillers were used in combination with the ceramic filler.

TABLE 3
PROPERTIES OF CERAMIC MICROSPHERES

Microsphere	Density (lb/ft ³)	Crush Strength (psi)
G200	156.1	60,000
G850	131.1	60,000

Nitric acid was used in the various functionalization processes along with thionyl chloride, dimethylformamide, diethyltoluenediamine, isoamyl nitrite. These were all obtained from Fisher Scientific. Two different surfactants BYK-Chemie 164 and 191 were used in the dispersion process.

2.2.2. Dispersion Methods

The simplest dispersion method used sonication and surfactants to improve the dispersion of the CNF in the Corfil 625-1. The surfactant-assisted dispersion method was conducted through six steps. First, pre-calculated amounts of Corfil 625-1 and CNF were carefully weighed, second, the CNF was sonicated using Fisher Scientific Sonic Dismembrator Model 100 in acetone to achieve the initial dispersion as shown in Figure 28, as the third step, surfactant was sonicated in acetone and added to the CNF mixture. The fourth step consisted of sonicating the CNF/surfactant mixture to reach the final dispersion state. Due to the thermal sensitivity of the as provided 625-1, adding resin to the mixture during sonication was not practical because the resin would start its curing cycle due to the heat generated in the sonication process. The acetone was then boiled out and the mixture stirred continuously using a magnetic stirrer resulting in a surfactant coated CNF residue. This was then added to the 625-1 and mixed. The six steps of the dispersion process are shown in Figure 29.



Figure 28. Sonicator used for processing.

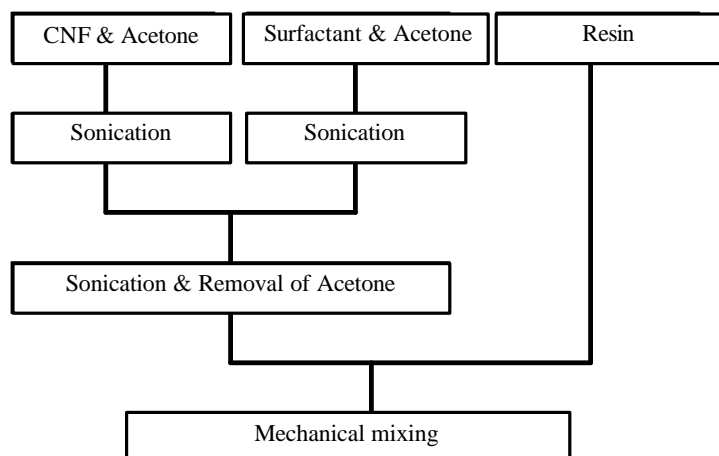


Figure 29. Sonication process.

Functionalization of the CNF involved sonicating in concentrated nitric acid for 30 minutes and refluxing at 120 C in order to produce the functional carboxylic acid group on the ends and at imperfections along the walls of the fiber. Figure 30 shows a representation of a carboxylic group attached to a carbon nanotube. 100 mL of acid was used for every gram of CNF and the mixture was refluxed for 4 hours. The nanofiber/acid solution was then filtered and the nanofibers washed to remove any remaining acid. The presence of the carboxylic group was verified through the use of infrared spectroscopy (Figure 31). The peak at 1730 cm^{-1} indicates the presence of the carbonyl group. After the CNF was functionalized, it was sonicated in acetone, and mixed with the potting compound with a method similar to steps 4-6 above.

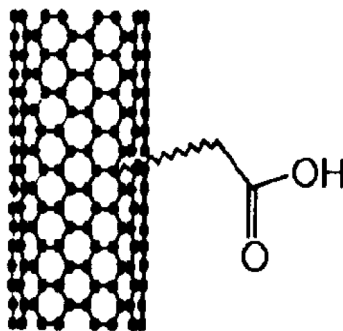


Figure 30. Representation of carbon nanotube functionalized with carboxylic acid group.

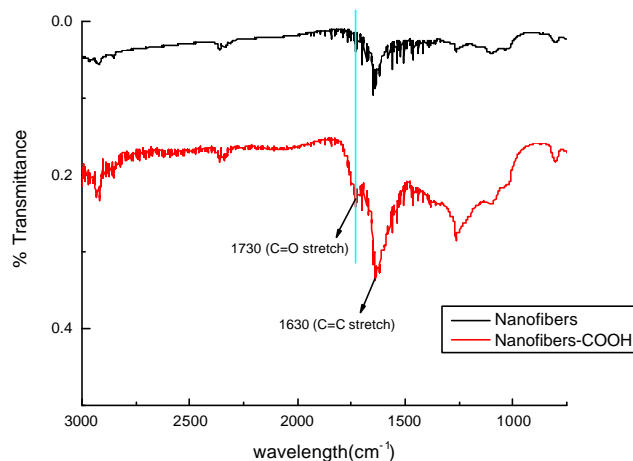


Figure 31. Infrared spectroscopy verification of carbonyl group.

A new processing technique was then developed in which the nanomaterials were initially dispersed in acetone using the sonicator and adding this dispersion to the potting compound base. The acetone was then removed by heating the mixture to just above the boiling point of the acetone (57 °C). This differs from the previous procedure in that the acetone is removed from the nanofibers after addition to the potting compound rather than before. This preserves the initial dispersion of nanomaterial in acetone and also allows for removal of all of the acetone. In the previous method, a nanofiber paste was produced by heating the nanofiber/acetone dispersion to remove enough acetone to maintain a paste that could be added to the potting compound. Once this paste was added, the remaining acetone could not be removed because the compound could not be heated without initiating curing. Pure acetone was added to the potting compound and then removed to determine if this procedure had any negative effects on the properties of the final compound. A test was also conducted to determine if applying vacuum to the prepared sample would remove entrapped air and enhance the properties

of the potting compound. These tests were used as controls to ensure that all changes were a result of the nanofiber added and not the procedure used.

This new processing technique was followed by various mixing procedures which included simple mechanical mixing using a laboratory mixer available from Cole-Parmer, an IKA homogenizer, and further sonication. The mixing times for the lab mixer and homogenizer were 30 minutes, while the sonication only method was performed for 5 hours.

To enhance the bonding of the nanomaterial with the potting compound functionalization to produce an amine group was performed. The amine group reacts with the epoxy group during the cure cycle to form cross-links between the polymer chains in the potting compound. Functionalization of the CNF involved sonicating and refluxing in concentrated nitric acid as discussed previously, producing the carboxylic acid group on the ends and at imperfections along the walls of the fiber. Thionyl chloride and diethyltoluenediamine (a common diamine curing agent) are then added to the CNF and stirred for 24 hours in an attempt to obtain an amine group at the end of the fiber. Another procedure involved adding Isoamyl nitrite and diethyltoluenediamine to raw CNF in dimethylformamide and stirring at 80°C for 3 hours. After functionalization, the CNF was mixed into the potting compound using the IKA homogenizer. A schematic of the aminofunctionalization is shown in Figure 32.

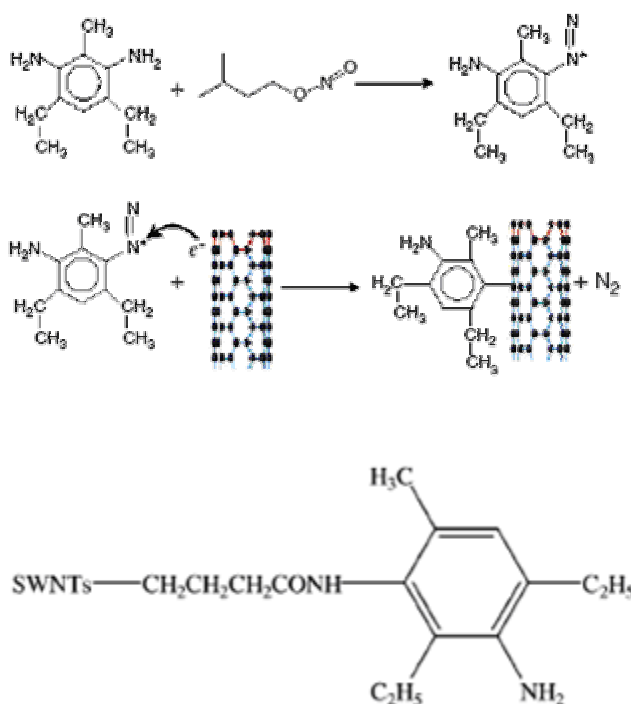


Figure 32. Schematic of amine functionalization procedures.

2.2.3. Test Methods

Prepared mixtures of nanomaterial and 625-1 were potted to produce both compression and lap shear test specimens. Compression samples were potted in cylindrical molds (0.5" diameter, 2.0" length) and cured at 350°F for 1 hour. After removing the specimens from the mold they were ground down to 1" length. The specimens were then tested according to ASTM D695-02a. Lap shear samples were prepared using aluminum coupons according to ASTM D1002 and cured at 350°F for 1 hour. Lap Shear testing is a cheap, simple way to determine the shear strength of adhesives and is representative of the core shear strength of a potting compound in honeycomb core. For each specimen a total of 6 compression samples and 7 lap shear sample were tested and an average was taken. The compression samples were used for density calculations.

The preparation method and amount of CNF in the first set of nanocomposites tested is summarized in Table 4. Specimens were examined with scanning electron microscopy (SEM) to see what effect the mechanical mixing had on the microballoons in the potting compound. Through the use of SEM it was determined that microballoons were being broken during the mixing process.

TABLE 4
SUMMARY OF COMPOSITES USED

Method	Functionalization	Surfactant 191	Surfactant 164	
CNF Weight % Used	1.5	1.5	1.5	3.0
		3.0		
	3.0	5.0	5.0	7.5

Compounds were then chosen for hot-wet testing which involved curing the samples as above and placing them in a humidity chamber for 30 days. The imposed conditions were 85% RH and 160 °F. After the treatment, the specimens were removed and the compression and lap shear tests performed at 180 °F. The specimens chosen for hot-wet treatment were 1.5% Surfactant 191, 3.0% Surfactant 164, 5.0% Surfactant 164, and 7.5% Surfactant 164.

Glass microballoons and ceramic microspheres from 3M were used in the potting compound that was provided by Cytec. These were hand mixed into the material that had no glass bubbles already present and then the curing agent was added. The glass and ceramic were added individually at various weight percentages and in combination to see if the high strength of the ceramic could be combined with the low density of the glass.

Multi-walled nanotubes were obtained in three different sizes ($<8\text{nm}$, $20\text{-}30\text{nm}$ and $>50\text{nm}$) and mixed into the potting compound with the laboratory mixer. The results were compared to determine the effect of nanotube size on the final properties of the composite.

Preliminary work was also conducted using an EXAKT Technologies three roll mill (Figure 33). This technology has previously been used in the paint and pharmaceutical industries to obtain controlled, even dispersions and has recently proven useful in the nanocomposites field. The three roll mill allows for control over the speed of the rollers, and the spacing between the rollers or the force between the rollers. This technology allows for high repeatability and can be scaled up for industrial use. Multi-walled nanotubes and buckyballs were mixed into the potting compound with the mill by running the material through the mill various times. In this investigation, the gaps and speed were kept constant while the number of times through was varied.

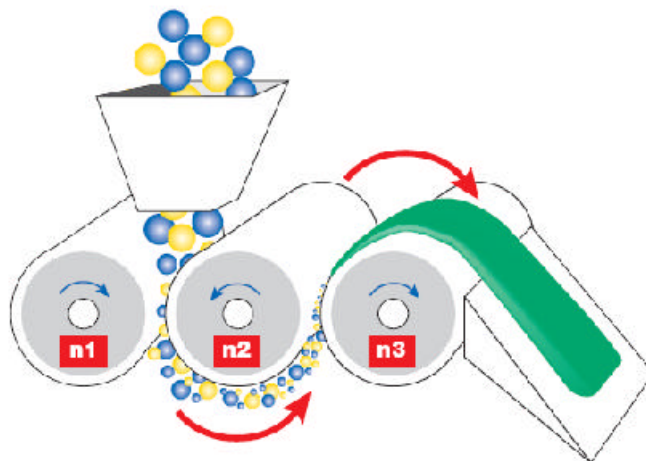


Figure 33. Schematic of Three Roll Mill from EXAKT Technologies.

CHAPTER 3

RESULTS AND DISCUSSION

3.1. SEM of Nanofibers and Glass Microballoons

After the first samples were mixed, SEM images were taken to determine what was happening at the micro and nanoscopic level within the potting compound. These images showing the initial CNF dispersion and broken microballoons can be seen in Figure 34. In image 1, a large group of CNF can be seen and image 2 gives a more magnified view. These pictures show the high level of clumping that exists when untreated CNF is added to the potting compound. This is not desired and actually decreases the strength of the material. When 1% untreated CNF was added to the potting compound, a decrease in compressive strength of 10% was observed. When 3% and 5% CNF was added, the resulting decreases were 22% and 17% respectively. Images 3 and 4 illustrate the broken state of the microballoons after initial mechanical mixing. This reduces the strength of the potting compound and also increases the density. In order to reduce breakage of the micro balloons, the shear force used in the mixing process was reduced and a flexible container was used.

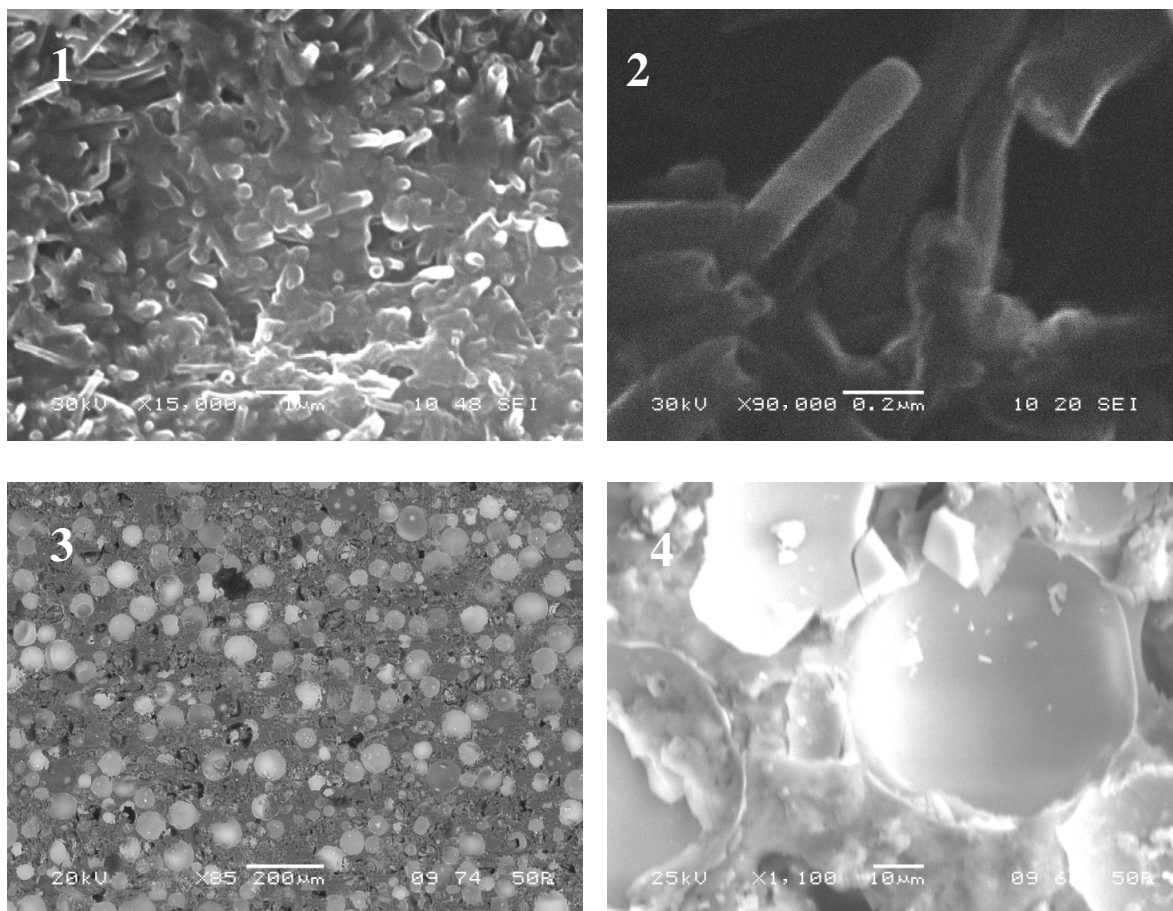
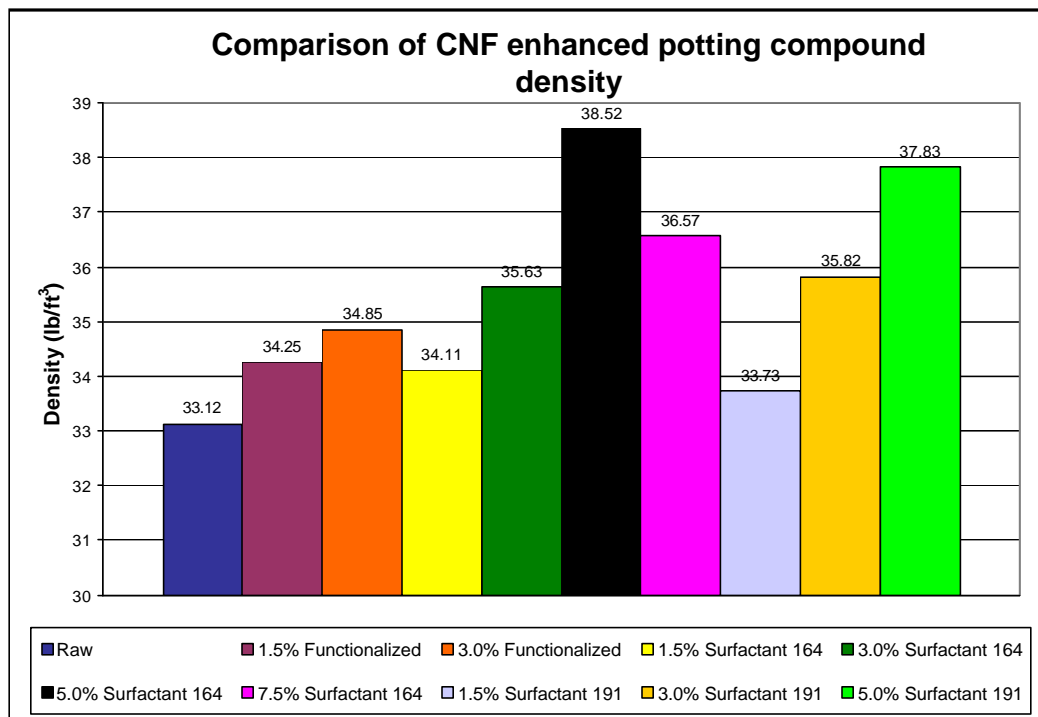


Figure 34. SEM images of potting compound with CNF (1) 15,000X view of CNF in potting compound (2) 90,000X close up of CNF aggregate (3) 85X view of microballoons in potting compound (4) 1,100X close up of broken microballoons.

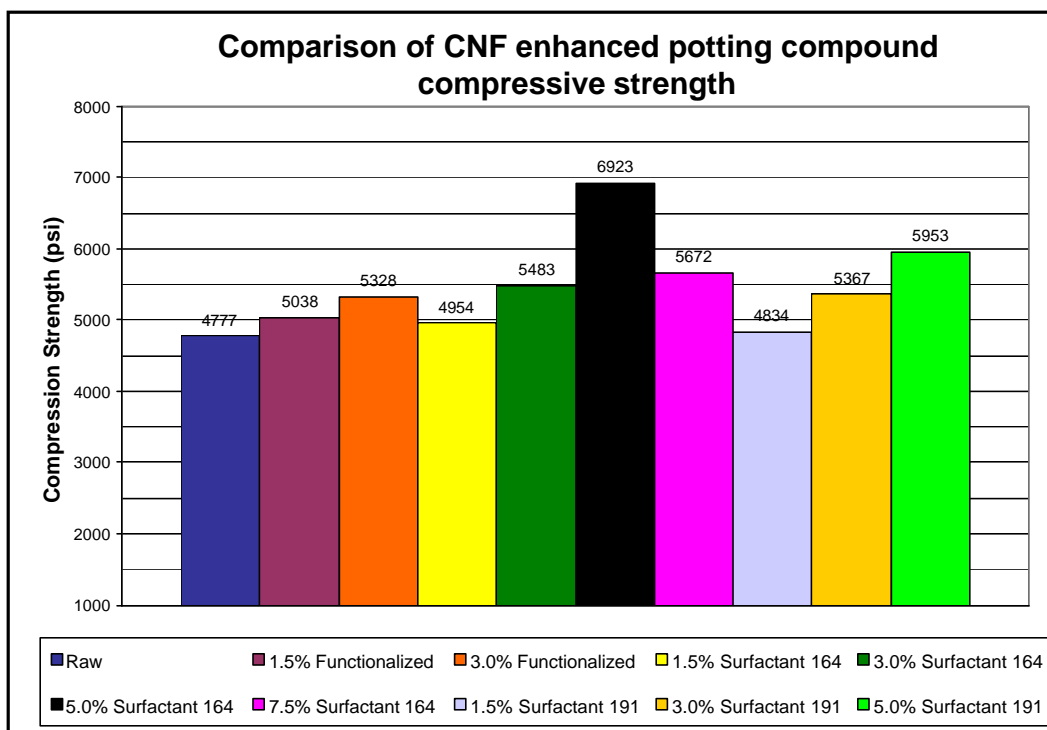
3.2. Functionalization and Surfactants

Figure 35 shows the test results for compounds in which carboxylic acid functionalization and surfactants were used (summarized in Table 4) along with the base 625-1 results. A relationship can be seen between the percentage of nanofiber added and all three of the measured properties. As the amount of nanofiber is increased, the density and compressive strength increases except for the case of 7.5 wt%+Surfactant 164. In terms of lap shear strength; the relationship is reversed, adding more nanofiber reduces the strength of the compound, again excluding the 7.5 wt%+Surfactant 164. The most promising results were obtained by using

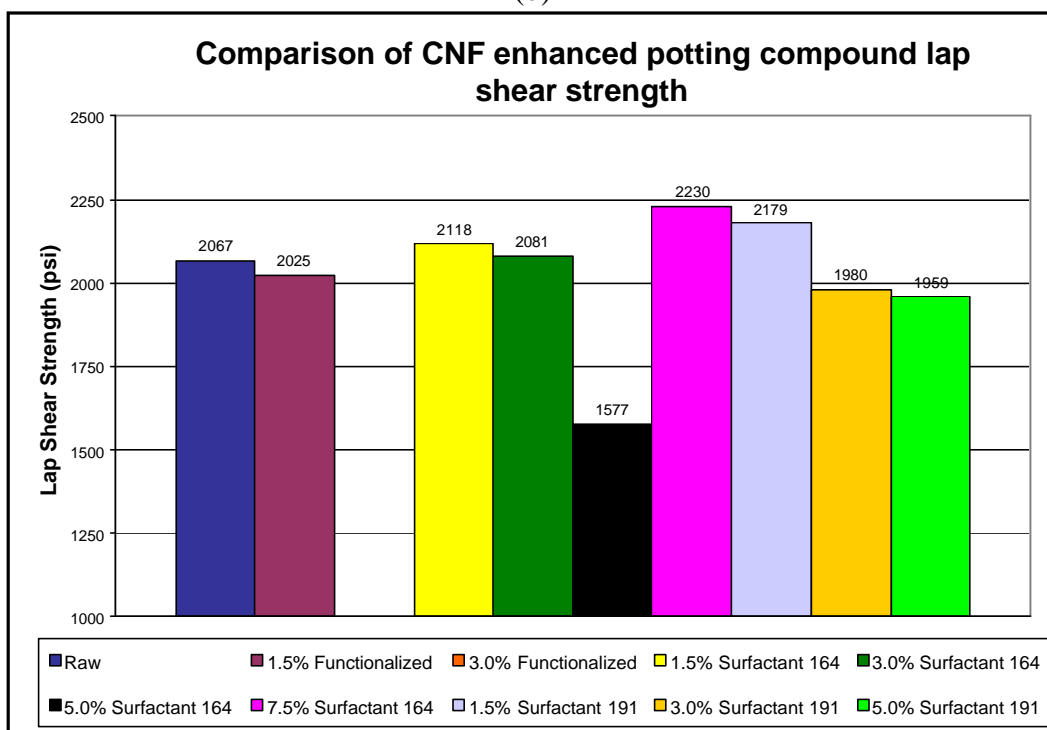
surfactant 164 with 5.0 wt% CNF. This resulted in an increase in compressive strength of 45% (from 4777 psi to 6923 psi) while the density of the material was only increased by 16% (33.12 lb/ft³ to 38.52 lb/ft³). The shear strength was reduced however from 2066 psi to 1577 psi (24%). This was not expected and is undesirable, but the lower shear strength is nearly identical to that of the EC-3500 compound currently used and is therefore acceptable. Increasing the amount of CNF beyond 5.0% using surfactant 164 did not result in further improvement as can be seen by the 7.5 wt%+Surfactant 164 which had a compressive strength 18% lower than the potting compound with only 5 wt% of nanofiber. It was not possible to add the functionalized nanofibers at higher percentages than 3 wt% because it became too dry and weak and the lap shear specimens were not testable. Surfactant 164 performed better in compression than surfactant 191 which shows that 164 interacts better with carbon nanofibers and can separate them more efficiently than 191.



(a)



(b)

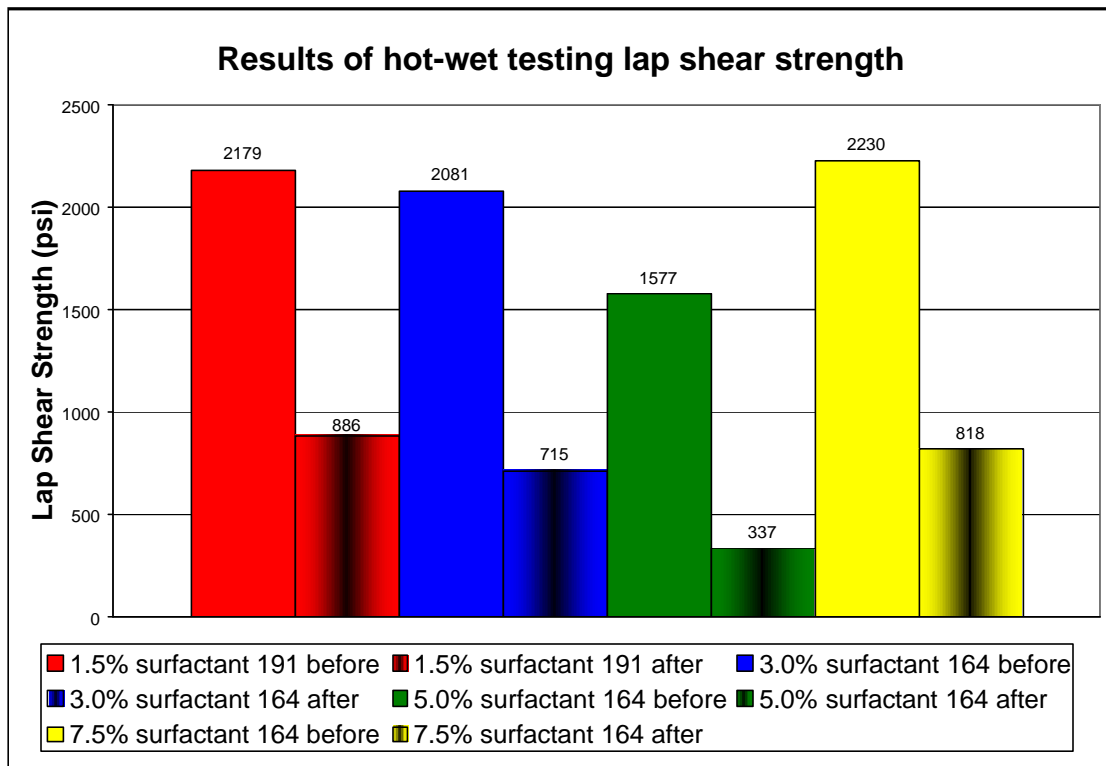


(c)

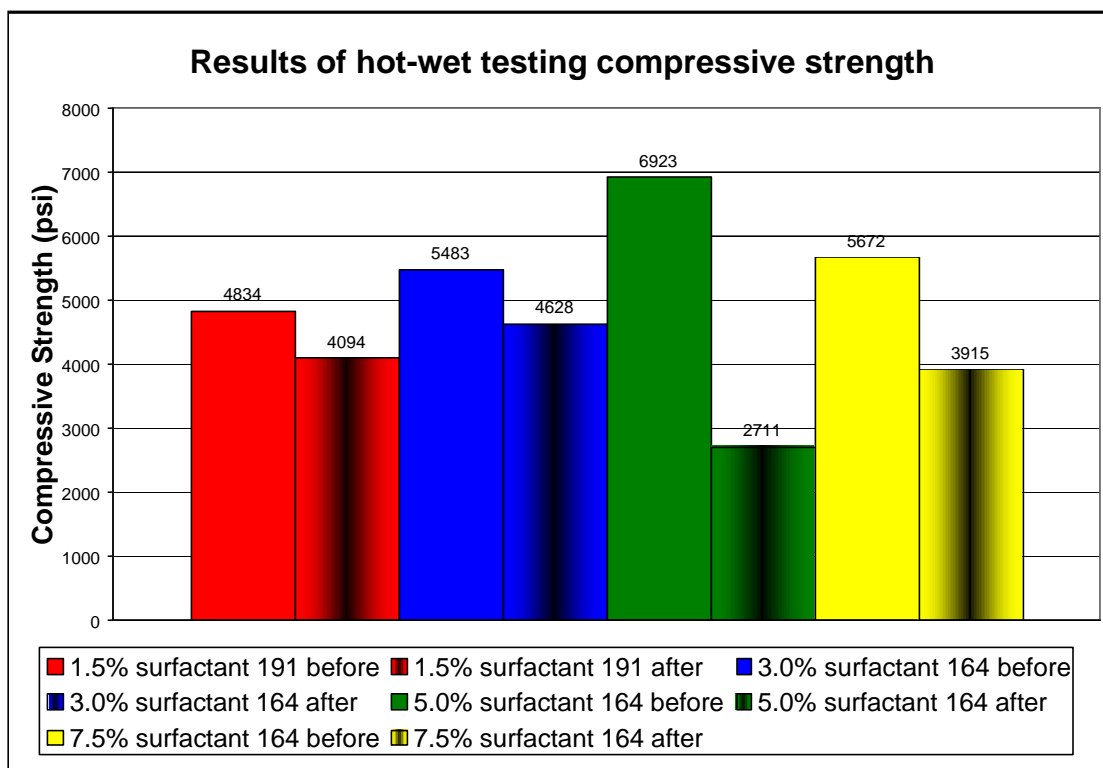
Figure 35. Summary of results obtained for all modified compounds (a) density, (b) compression strength, (c) lap shear strength.

3.3. Hot Wet Testing

The following surfactant/CNF combinations were conditioned in 85% RH at 160 °F for 30 days and then tested at 180 °F: 1.5%+Surfactant 191, 3.0%+Surfactant 164, 5.0%+Surfactant 164, and 7.5%+Surfactant 164. The goal was to see the effect of the CNF percentage on the hot/wet properties of the potting compound. Results of the hot/wet testing can be seen in Figure 36. An average decrease in lap shear of 67% was observed for the 4 compounds tested. This is much higher than the 14% lost by the 625-1 as provided by Cytec. The 5.0%+Surfactant 164 showed the highest loss in properties, the compressive strength was reduced by 61% and the lap shear was reduced by 78%. The 3.0%+Surfactant 164 maintained the highest compressive strength after hot-wet testing at 4628 psi.



(a)



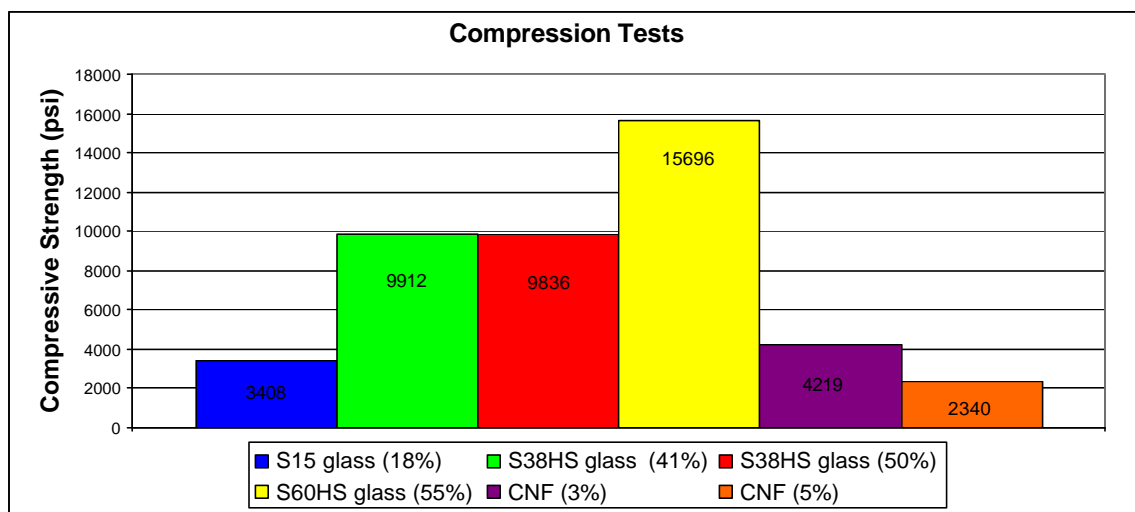
(b)

Figure 36. Results of hot-wet testing (a) lap shear strength, (b) compressive strength.

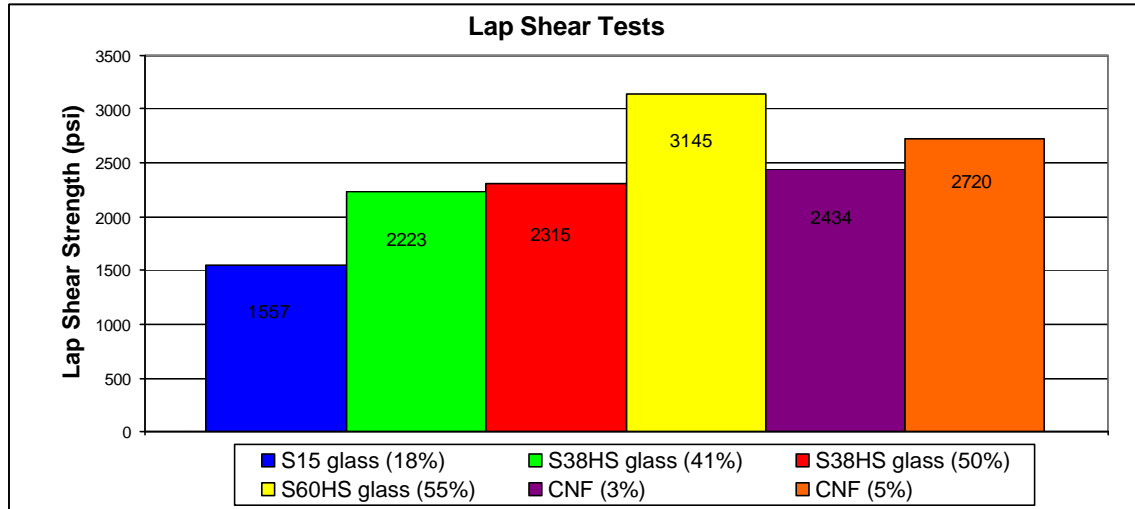
3.4. Investigation of New Glass Microballoons

Three different glass microballoons were used from 3M in the base resin provided by Cytec to obtain a compound similar to the 625-1. Tests were also conducted to determine if the desired potting compound properties could be obtained through the use of microballoons alone. The results are shown for compounds containing 18 wt% of the lowest density microballoon (S15), 41 wt% and 50 wt% of the medium density microballoon (S38HS), and 55 wt% of the high density microballoon (S60HS). The high strength of the potting compound containing S60HS (15,700 psi) shows that it is possible to obtain the desired strength in a one-part compound, however the density (52 lb/ft³) is nearly double what is desired. The compound obtained with the S15 microballoon gives results very similar to those of the standard 625-1 with a density of 32 lb/ft³, compressive strength of 3,400 psi, and lap shear strength of 1,550 psi. This

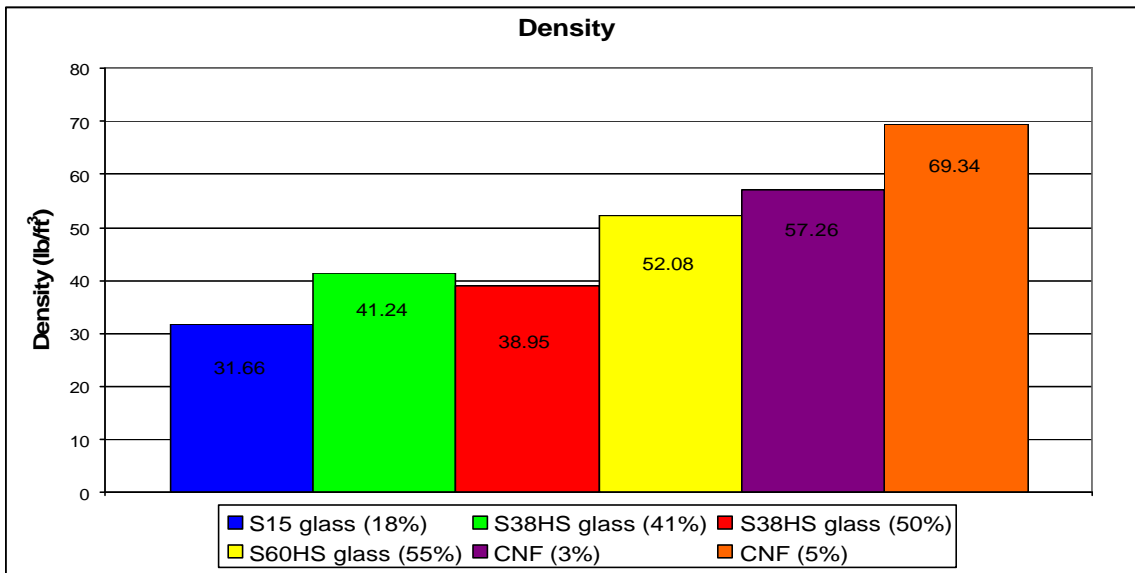
compound was chosen as the standard to measure improvements of compounds that contain nanomaterials. The S38HS microballoons showed the desired strength of 9900 psi with a density of 39 lb/ft³, this is not as low as 625-1; however, it is comparable to EC-3500 in the desired form of a one-part potting compound. This formulation could be used to replace EC-3500, giving the same performance while eliminating the hassles associated with a two-part material. Results for the different microballoons are shown in Figure 37. This figure also shows the results of adding CNF without any glass filler. CNF (3 wt% and 5 wt%) was dispersed in the base resin using a surfactant, cured and tested. Results show the very high density that is obtained without the hollow glass spheres. It is also seen that the compressive strength is lower than that obtained with the weakest microballoon. The only property that is improved is the lap shear strength showing an increase of 75% to 2700 psi at 5 wt%. This shows the potential for strength enhancement using the carbon nanofibers, however, methods to improve the dispersion need to be developed to increase the compressive strength and lower the density.



(a)



(b)



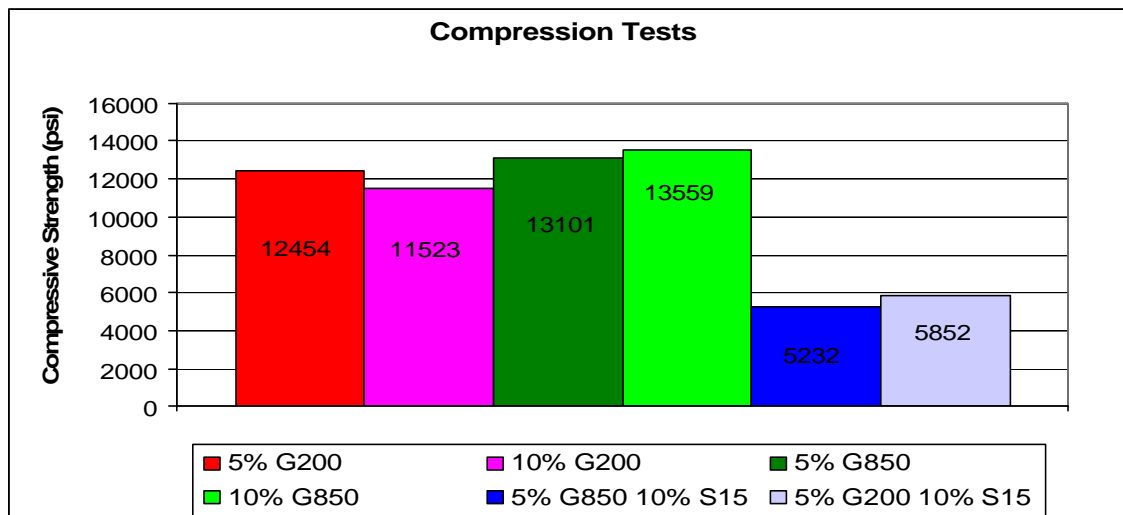
(c)

Figure 37. (a) Compression results for glass microballoons, (b) Lap Shear results for glass microballoons, (c) Density results for glass microballoons.

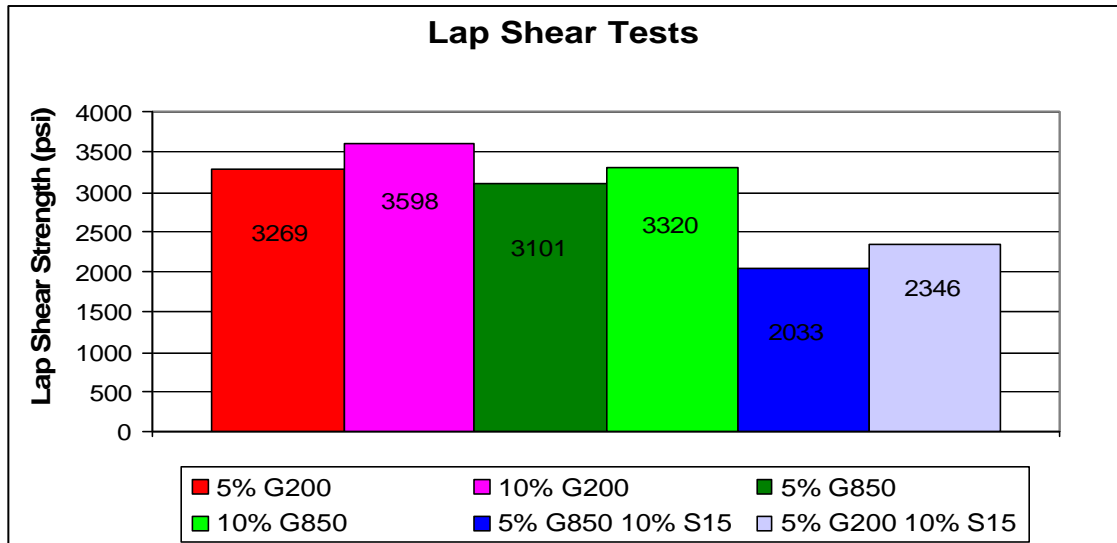
3.5. Investigation of Ceramic Microspheres

Results for the addition of the ceramic microspheres are shown in Figure 38. Addition of both kinds yields a great increase in compressive strength, lap shear strength and density. The G200 microspheres gave a compressive strength of 12,000 psi, lap shear strength near 3,500 psi and a density of 69 lb/ft³. Addition of the G850 ceramic microspheres resulted in a compressive

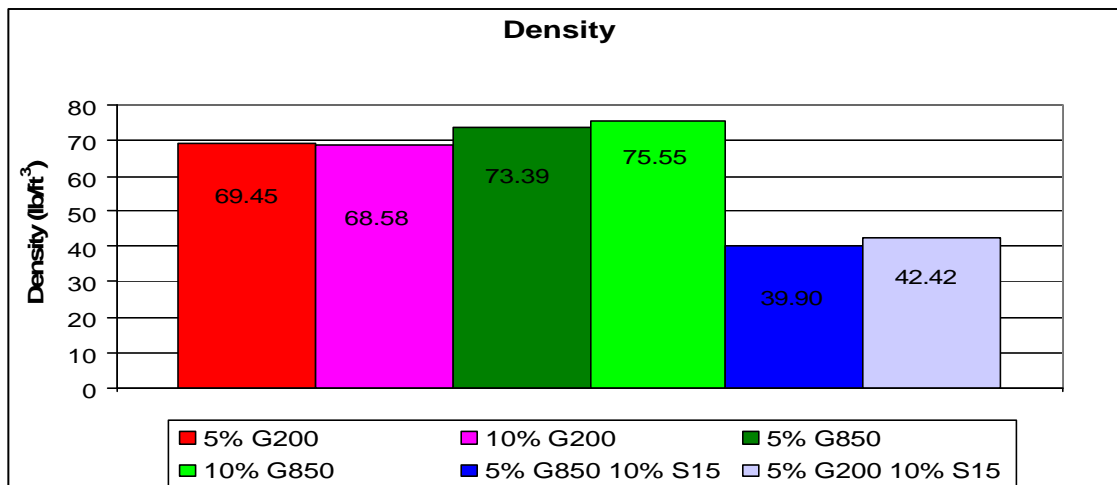
strength of 13,000 psi, lap shear strength of 3,200 psi and a density of 74 lb/ft³. The density of both compounds is too high to be used in the desired application, so some of the lowest density glass microballoons were added to reduce the overall density of the potting compound. When 10 wt% S15 is added along with 5 wt% of G200, the density is lowered significantly, but so are the compressive and lap shear strengths. The density (42 lb/ft³) is similar to that obtained previously using the S38HS microballoons, but the compressive strength is nearly half at 5,200 psi. Results are nearly identical when 10 wt% S15 is added along with 5 wt% G850. The same trend can also be seen when different density microballoons are added together. The failure of the potting compound is determined by the weakest microballoon present in the material. The key to obtaining the desired material with low density and high strength is finding a material that will handle the entire load with the microballoons only functioning as density reducers, not carrying any of the load.



(a)



(b)



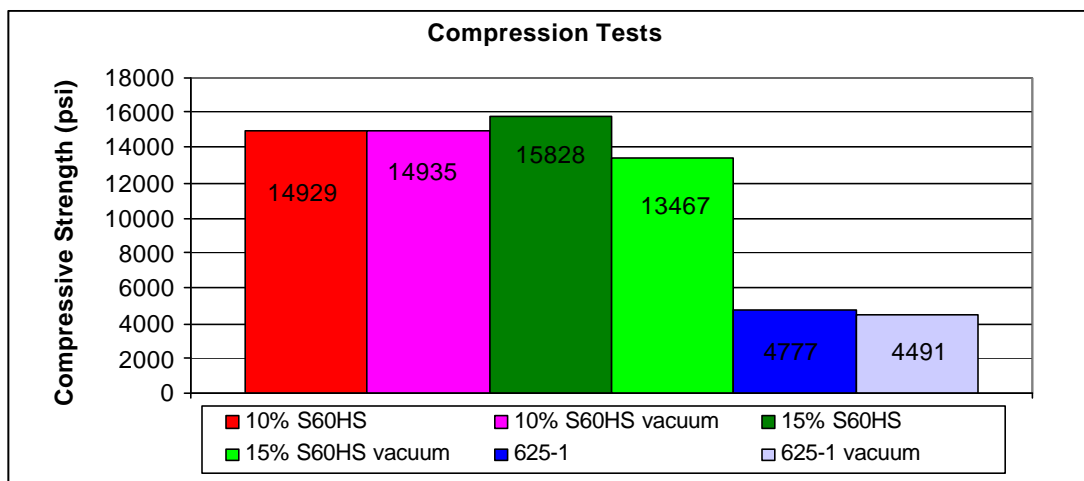
(c)

Figure 38. (a) Compression results for Ceramic Microspheres, (b) Lap Shear results for Ceramic Microspheres, (c) Density results for Ceramic Microspheres.

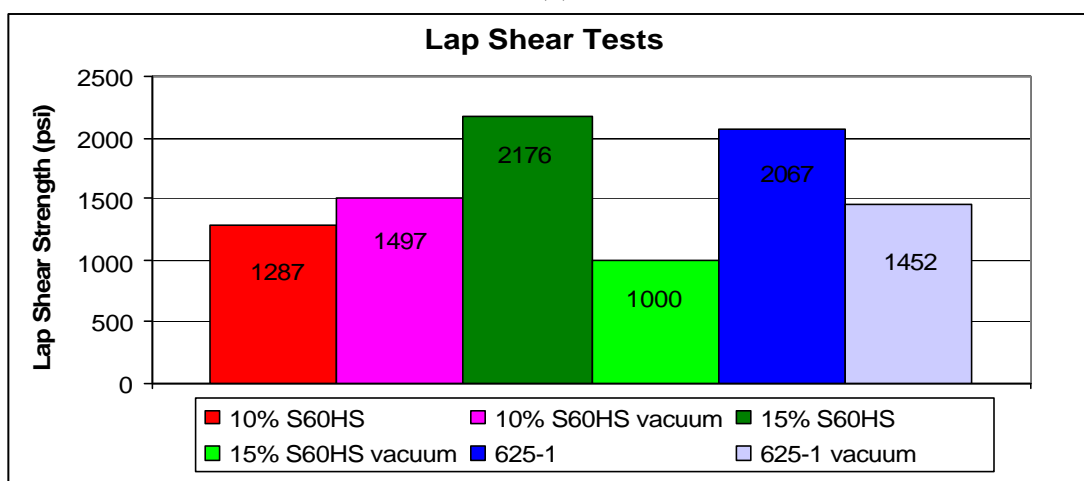
3.6. Application of Vacuum to Samples

In order to determine if excess air was being added during the mixing process, vacuum was applied to three different samples, two containing the high strength glass microballoons and the base 625-1, after processing and compared with samples in which no vacuum had been applied. If air is being added during mixing, the strengths and density of the potting compound could possibly be reduced. Although it is desirable to have low density, it is not acceptable to

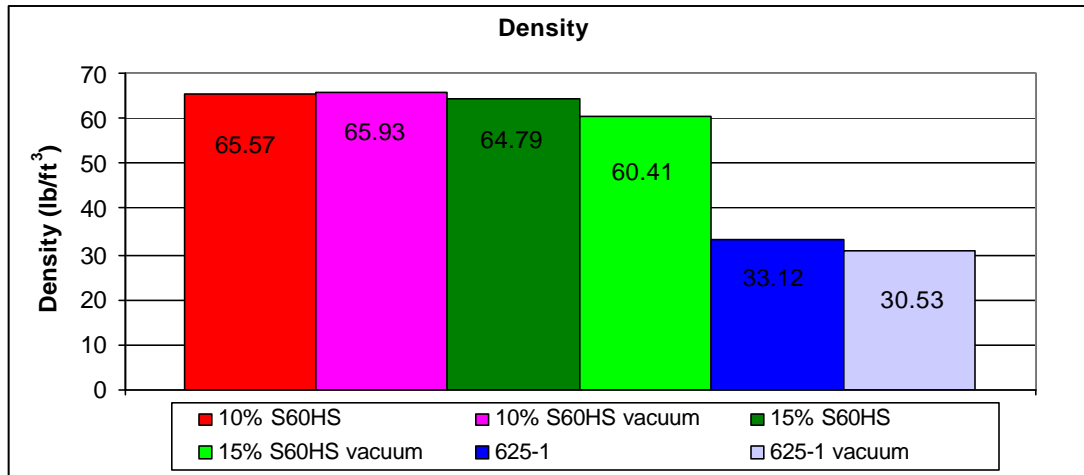
have the strength reduced because of the added air. The addition of air also reduces the consistency of the mixing process. Results for the tests are shown in Figure 39. The vacuum had little effect on the compound containing 10% S60HS, with no change in compressive strength or density and a slight increase in lap shear strength. It can be seen that for the cases of 15 wt% S60HS and the standard 625-1 the density is lowered by roughly 7% which is desired, however the compressive and lap shear strengths of the material are also lowered. It was thus concluded that no vacuum would be applied to the potting compound before it was cured because the decrease in density was not high enough to accept the decrease in strengths.



(a)



(b)



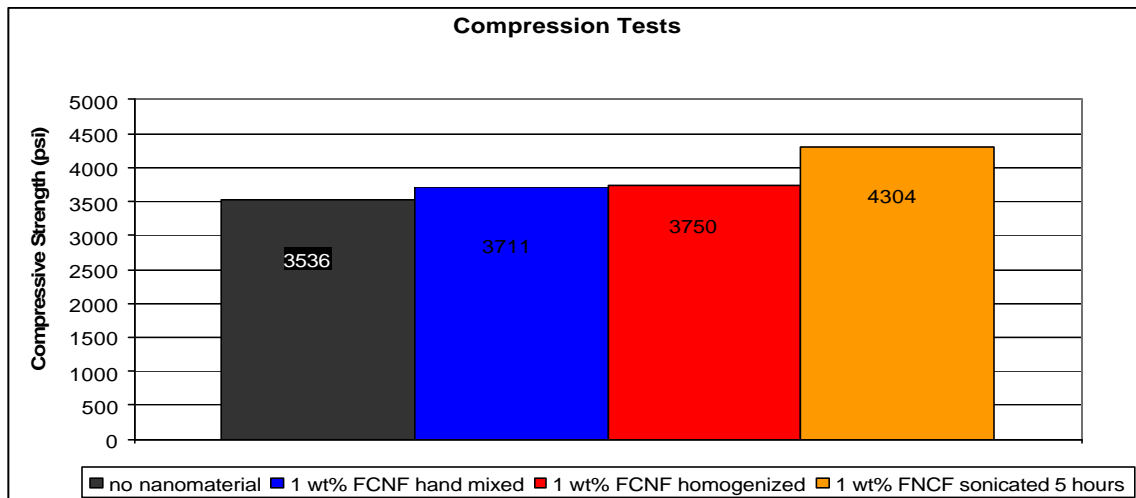
(c)

Figure 39. (a) Compression results for applying vacuum, (b) Lap Shear results for applying vacuum, (c) Density results for applying vacuum.

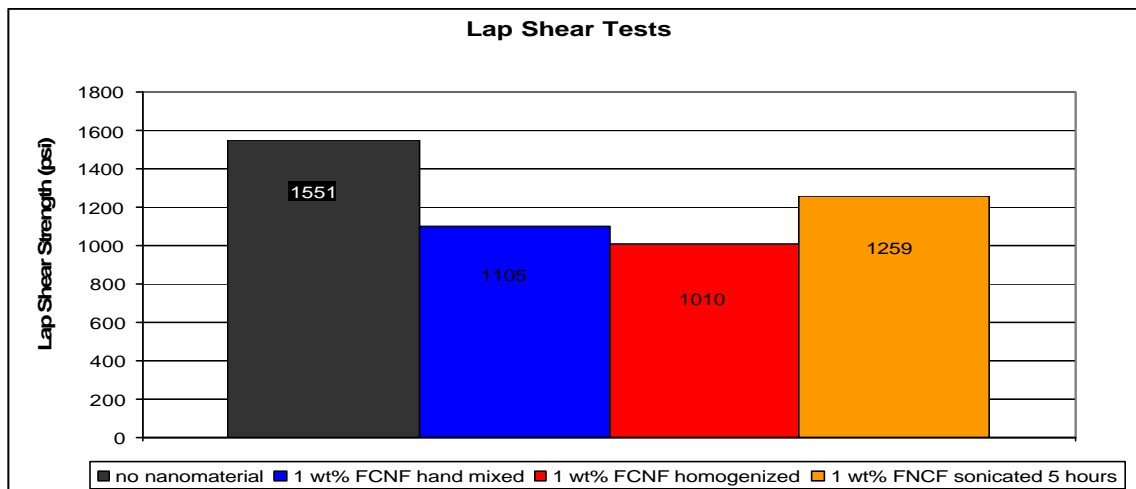
3.7. New Processing Methods

The results of the new processing method are presented in Figure 40. The acetone was removed after addition to potting compound and mixing by lab mixer, homogenizer, and sonication. The last two mixing methods were not previously possible because of the high viscosity of the potting compound without the acetone present. All mixing methods show improvement in compressive strength over the base material. Hand mixing and homogenization showed only a very slight increase in compressive strength (2%) while the highest improvement is seen when the sample is sonicated for 5 hours followed by removal of the acetone. An increase of 21.7%, from 3,536 psi to 4,304 psi, is obtained by this method. A decrease is seen in the lap shear strength for all methods, but the lowest decrease (18.8%) is observed for the sonication mixing method. The density of the sonicated potting compound is higher than the base by 9.7% so to fairly measure the increase in compressive strength, the compressive strength is divided by the density for all mixing methods and presented in the last graph of Figure 40. This still shows an improvement of 10.9%. The sonication method is most effective because it provides enough

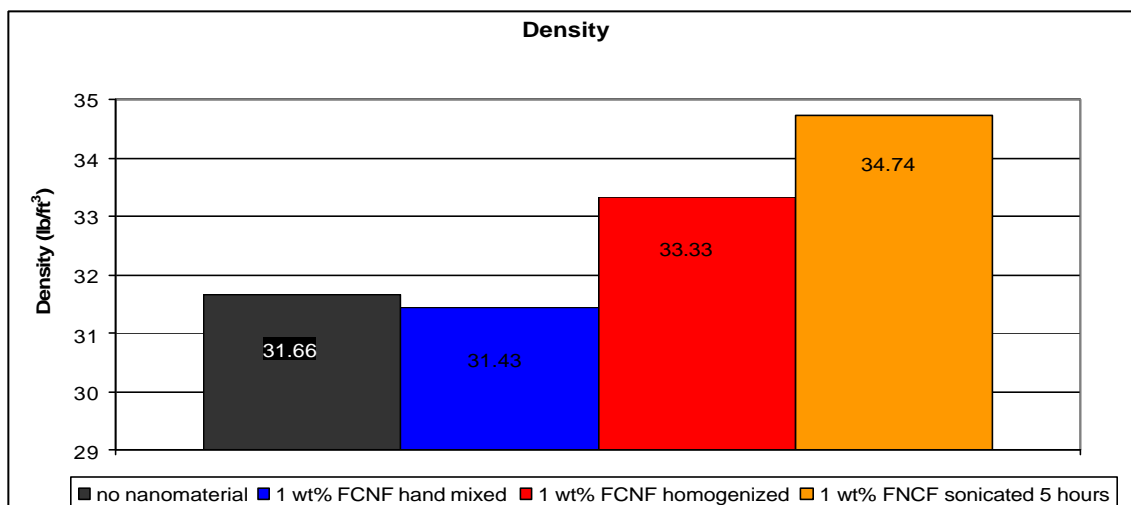
energy to break apart the CNF aggregates without damaging the individual fibers as much as the homogenization.



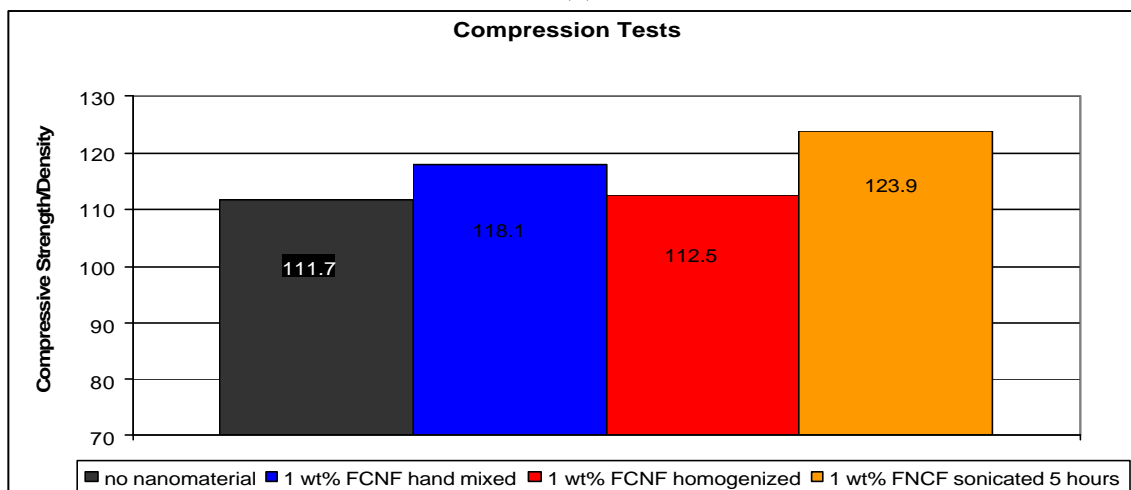
(a)



(b)



(c)



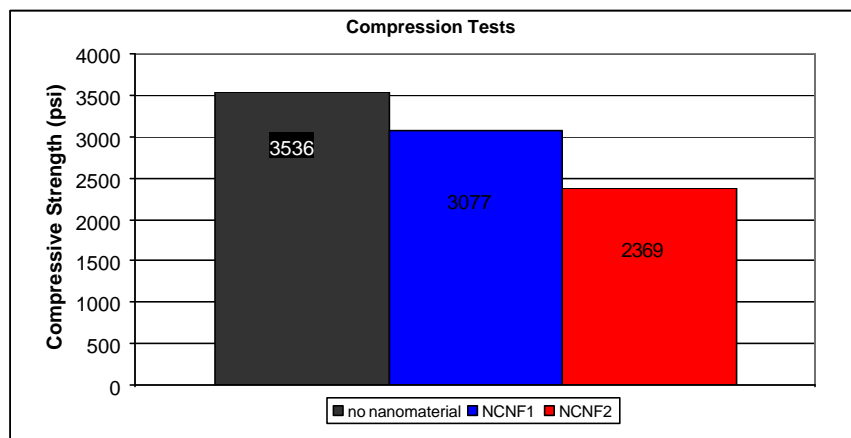
(d)

Figure 40. (a) Compression results for new processing method, (b) Lap Shear results for new processing method, (c) Density results for new processing method, (d) Compression/Density results for new processing method.

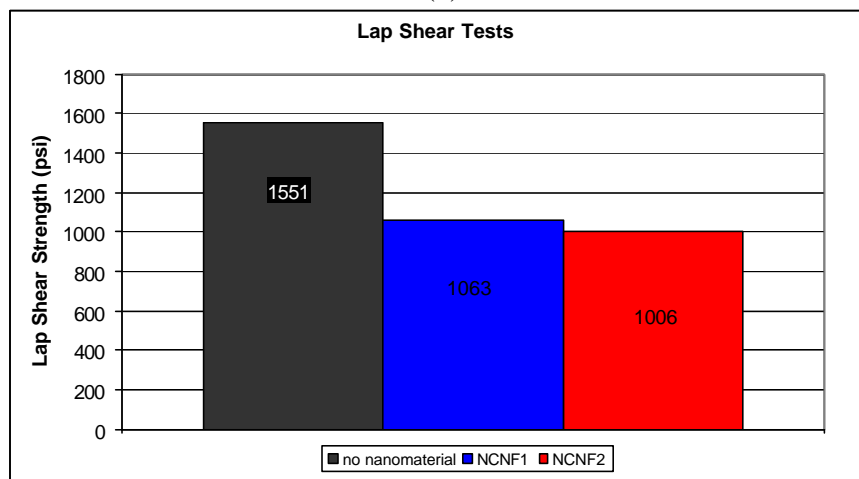
3.8. Amine Functionalization

Two methods were used in an attempt to add the amine functional group to the CNF. The results of both methods are shown in Figure 41. Both functionalization methods showed a decrease in all properties. The lap shear strengths decreased by 33% for both methods while compressive strength decreased by 13% for method 1 and 33% for method 2. Fibers from both methods were analyzed by FTIR and the amine group was not found in the analysis. The fibers

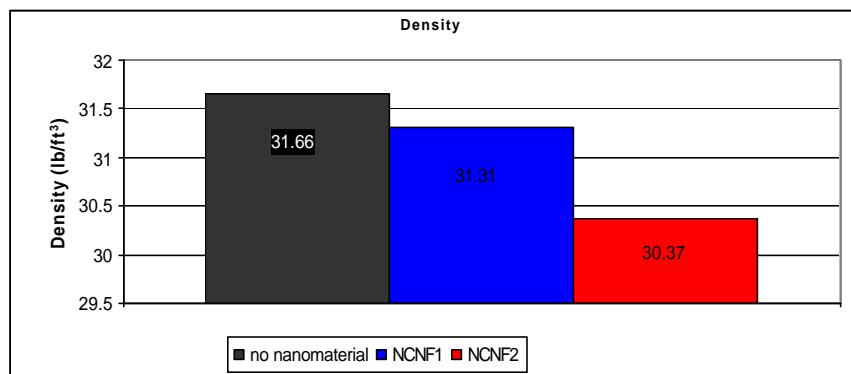
were damaged by the functionalization processes resulting in the lowered properties. This shows that further functionalization work needs to be done as there could be great benefits if the nanomaterial contains an amine group which can be covalently bond with the potting compound.



(a)



(b)

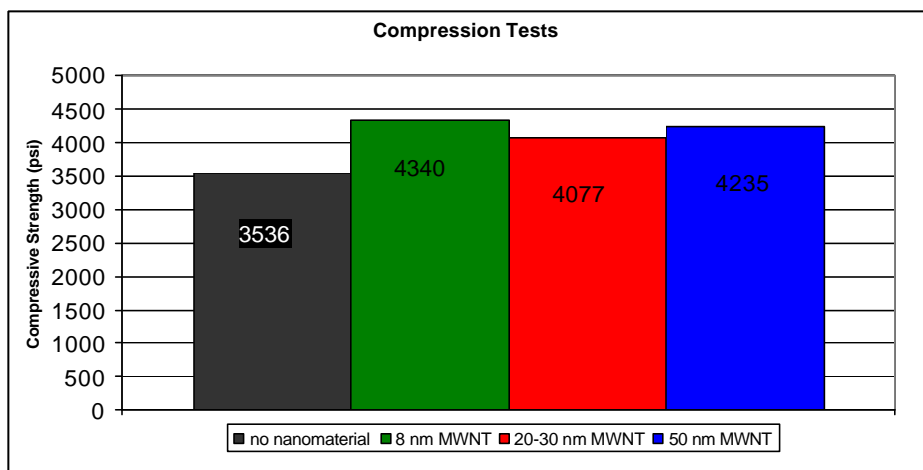


(c)

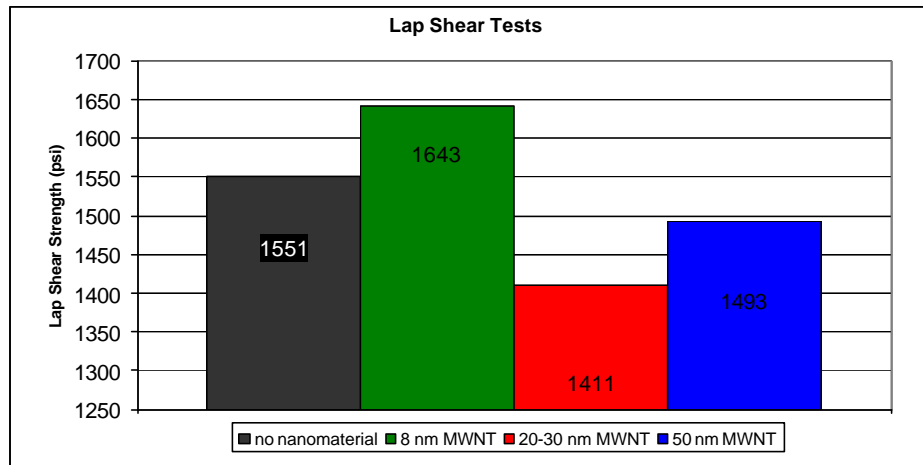
Figure 41. (a) Compression results for amine functionalization, (b) Lap Shear results for amine functionalization, (c) Density results for amine functionalization.

3.9. Use of MWNT

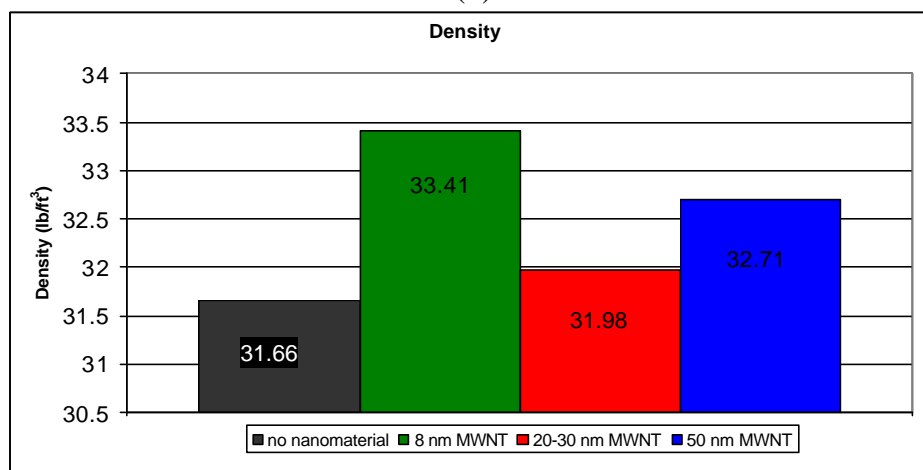
MWNT were used in three different sizes, 8 nm, 20-30 nm, and 50nm. All three sizes of MWNT showed an increase in the mechanical properties of the potting compound. The compressive strength was similar for all three sizes; however, the lap shear strength decreased for all except the smallest MWNT. The medium size nanotube showed an increase of 15.3% in compressive strength and a decrease of 9% in lap shear. A 22.7% (4340 psi from 3536psi) increase was obtained using the 8 nm MWNT and a 5.9% increase in lap shear was obtained using the same MWNT. The largest nanotube gave an increase of 19.8% in compressive strength and a decrease of 3.7% in lap shear. The density of the 8 nm nanotube increased by 5.5%, the 20-30 nm tube remained the same, and the 50 nm MWNT increased by 3.3%. When taking the density increase into account by dividing the strength by the density to obtain a specific strength, an overall improvement of 16.3% is seen for the 8 nm MWNT in compression and no change is seen in lap shear. The specific compressive strengths are nearly identical for all sizes of nanotube; however, the specific lap shear is significantly lower for the two largest nanotubes. The results for all MWNT are shown in Figure 42.



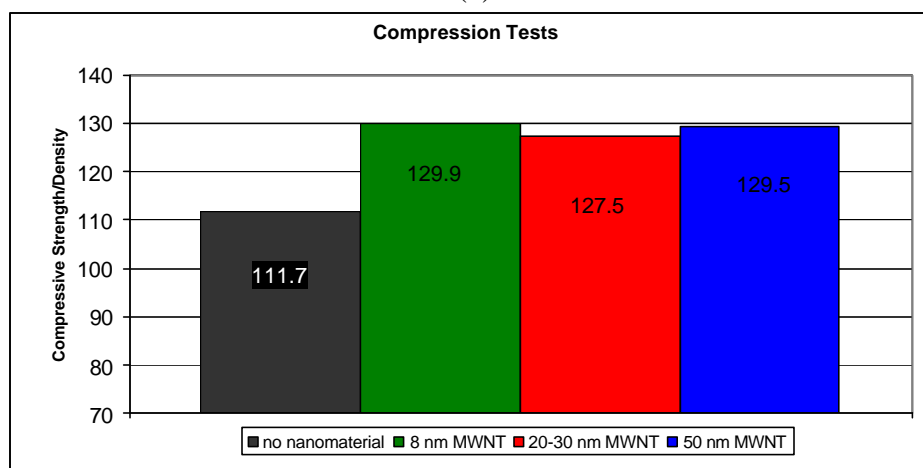
(a)



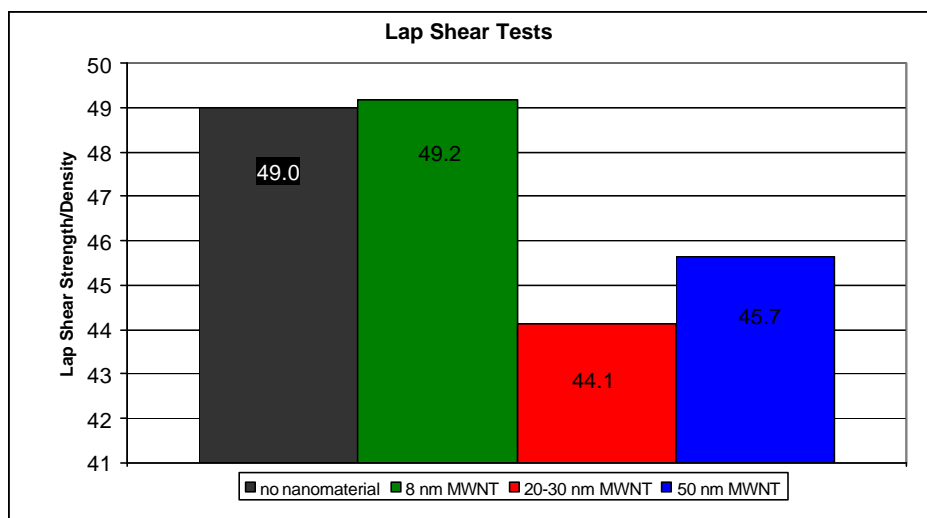
(b)



(c)



(d)



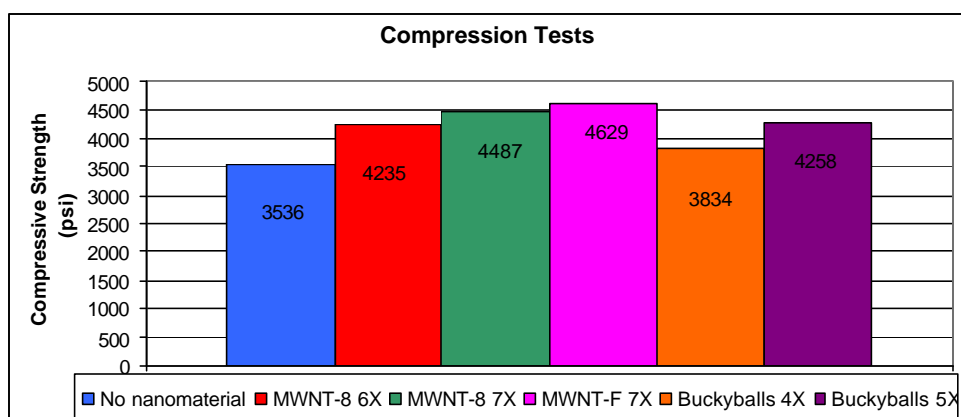
(e)

Figure 42. (a) Compression results using MWNT, (b) Lap Shear results using MWNT, (c) Compression/Density results using MWNT, (d) results using MWNT, (e) Lap Shear/Density results using MWNT.

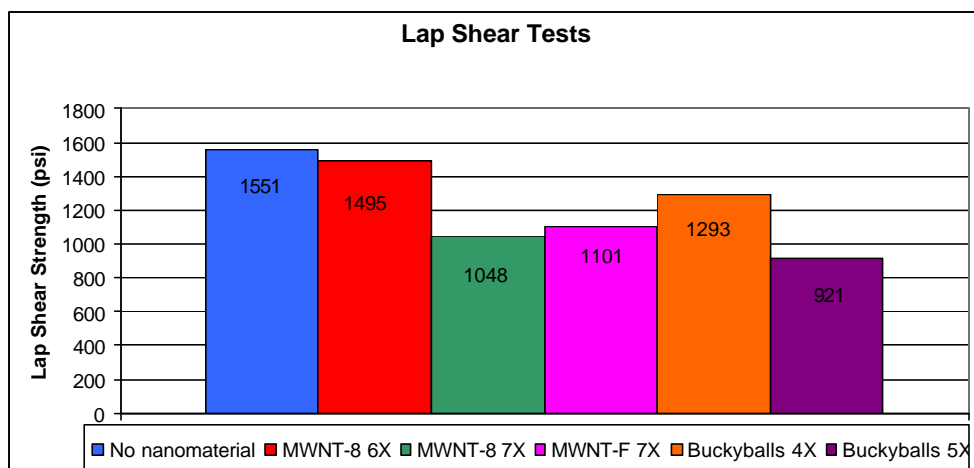
3.10. EXAKT Three Roll Mill

The EXAKT Technologies 80E three roll mill was used to run samples and determine the potential of the machine for use in dispersing nanomaterials into the potting compound. The device requires much less preparation than the previously mentioned mixing techniques and is more scalable to the industrial environment. Results using 1 wt% 8 nm MWNT, carboxylic acid functionalized 20-30 nm MWNT, and buckyballs are presented in Figure 43. An increase in compressive strength is seen in all of the potting compounds mixed with the three roll mill with the greatest increase coming from the functionalized MWNT. The 20-30 nm functionalized nanotubes increased the compressive strength of the potting compound from 3536 psi to 4629 psi or 30.9%. A decrease in lap shear strength was observed for all the samples. Two samples of the 8 nm MWNT were produced, one going through the mill 6 times and one going through 7 times. The compressive strength of the sample that went through 7 times (4487 psi) is higher than the sample that went through only six times (4235 psi). The same is true for the buckyballs; the

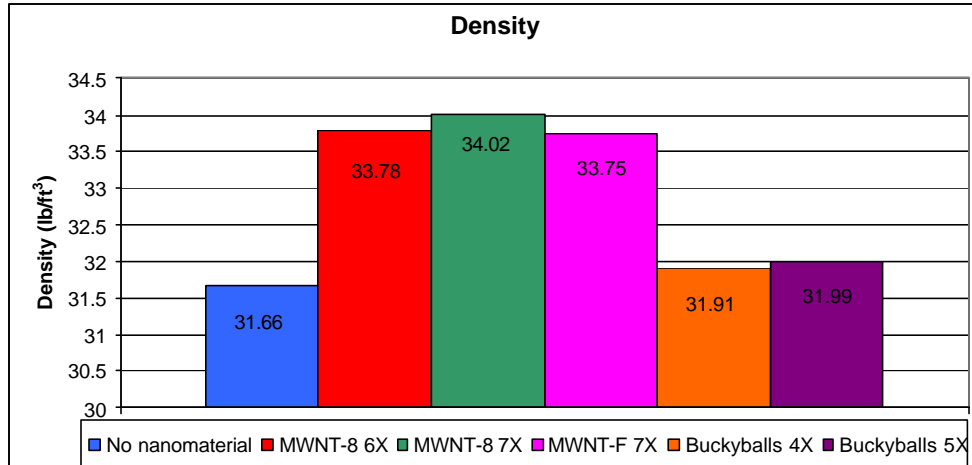
sample that went through 5 times had higher compressive strength (4258 psi) than the sample that went through only 4 times (3834 psi). This shows the dependence of properties on the number of times through the mill and the need to optimize the procedure to obtain the best properties possible. The densities of the compounds with nanotubes are roughly 7% higher than that of the raw 625-1, while the densities of the compounds containing buckyballs are only 1% higher. The compound with the functionalized nanotubes, the one with the greatest strength improvement, has a density which is 6.6% higher. The specific compressive and lap shear strengths are shown in Figure 43 to account for the density increases in all of the materials. The 20-30 nm functionalized fibers yielded an increase of 22.8% in specific compressive strength.



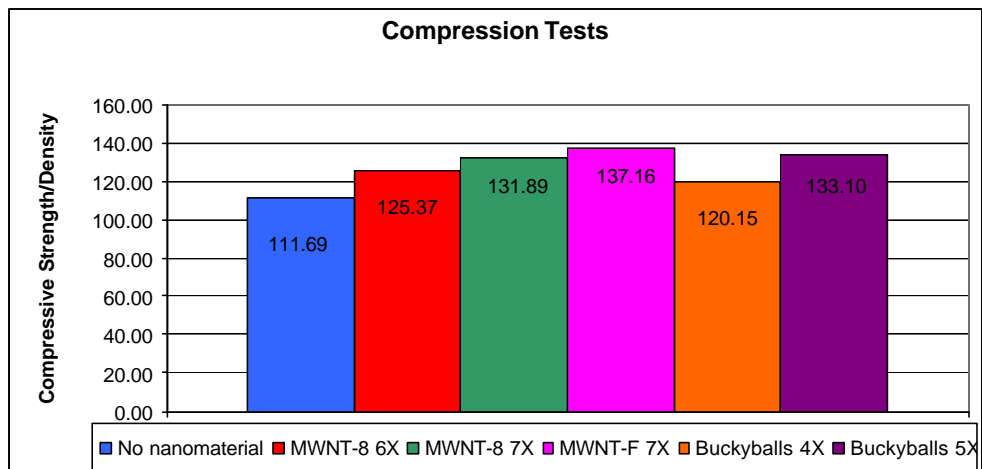
(a)



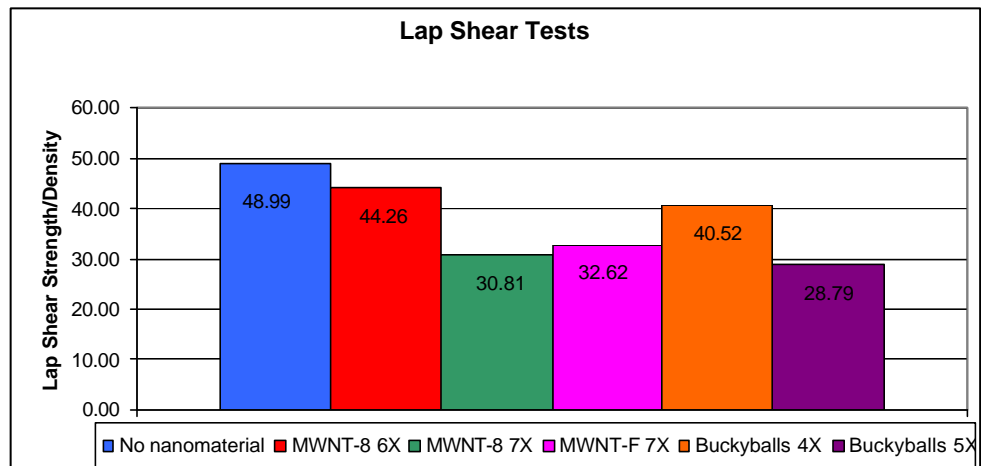
(b)



(c)



(d)



(e)

Figure 43. (a) Compression results using three roll mill, (b) Lap Shear results using three roll mill, (c) Density results using three roll mill, (d) Compression/Density results using three roll mill, (e) Lap Shear/Density results using three roll mill.

CHAPTER 4

CONCLUSIONS

The potential for strength enhancement of potting compounds by adding small amounts of carbon nanomaterial, including carbon nanofibers, multi-walled nanotubes and buckyballs, has been shown. The composite materials are improved because of the unique properties of the nanomaterials. Difficulties however are presented in the form of dispersion of the nanomaterial within the matrix and bonding with the matrix to allow load transfer. Several methods were developed to overcome these difficulties and produce a higher strength one-part potting compound. Specimens were prepared to be tested for lap shear and compressive strengths and the density of each sample was calculated.

Surfactants and functionalization (with carboxylic acid and amine functional groups) were shown to have an effect on the final strength of the material. The use of a surfactant produced the highest increase in compressive strength while the attempted functionalization with an amine reduced the mechanical properties of the composite. Glass microballoons and ceramic microspheres have also been used to modify the properties of the compound. The glass microballoons allow for control over the potting compounds density and show that a one-part compound can be attained with properties equivalent to the two-part potting compound EC-3500. Potting compounds with a wide range of densities and strengths can be produced by selecting a certain type of glass balloon and the amount that is added. Although ceramic microspheres are a high strength additive, they are not suitable for use in this potting compound because of the high density they give to the potting compound. Processing methods have been developed which lead to further enhancement of the mechanical properties of the 625-1 potting compound. These

methods consisted of mechanical mixing, homogenization, sonication and three roll milling. Sonication produced the greatest increase in strength compared to basic mixing and homogenization. Three roll milling is the simplest and most scalable of all the methods, and it was shown that the number of times the material is passed through the mill has an effect on the strength of the resulting material. The compressive strength was higher when the MWNT were run through the mill 7 times as compared to only 6. Another important factor in the improvement of the potting compound is the amount of nanomaterial added. The properties increase as the amount of filler is increased up to a certain weight percentage. After this optimum is reached, further addition leads to a decrease in compressive strength.

With further investigation into the functionalization of the nanomaterials and knowledge of the interaction between the potting compound resin system and the chemical groups on the nanomaterial, an ideal nanomaterial can be produced that will provide the greatest strength enhancement. When this is combined with the optimum dispersion method and amount of filler, the benefits of carbon nanomaterials can be fully realized.

REFERENCES

REFERENCES

- [1] Kroto HW, Heath JR, O'Brian SC, Curl RF, Smalley RE. C_{60} : Buckminsterfullerene. *Nature* 1985; 318(6042): 162-163.
- [2] Fuller RB. *The Artifacts of R. Buckminster Fuller: A Comprehensive Collection of His Designs and Drawings*, ed. W. Marlin, Garland, New York, New York, 1984.
- [3] David W, Ibberson R, Matthewman J, Prassides K, Dennis T, Hare J, Kroto H, Taylor R, Walton D. Crystal Structure and Bonding of Ordered C_{60} . *Nature* 1991; 353(6340):147-149.
- [4] Stephens PW, Mihaly L, Lee PL, Whetten RL, Huang SM, Kane R, Deiderich F, Holczer K. Structure of single-phase superconducting K_3C_{60} . *Nature* 1991; 351(6328):632-634.
- [5] Guozhong C. *Nanostructures and Nanomaterials: Synthesis, Properties and Applications*. Imperial College Press 2004, London, UK.
- [6] Diederich F, Whetten R. Beyond the C_{60} : The Higher Fullerenes. *Acc. Chem. Res.* 1992; 25:119-126.
- [7] Smalley RE. Self-Assembly of the Fullerenes. *Acc. Chem. Res.* 1992; 25(3):98-105.
- [8] Krätschmer W, Lamb LD, Fostiropoulus K, Huffman DR. Solid C_{60} : a new form of carbon. *Nature* 1990; 347(6291): 354-358.
- [9] Kortan AR, Kopylov N, Glarum S, Gyorgy EM, Ramirez AP, Fleming RM, Thiel FA, Haddon RC. Superconductivity at 8.4 K in calcium-doped C_{60} . *Nature* 1992; 355(6360): 529-532.
- [10] Dresselhaus MS. Future Directions in Carbon Science. *Annu. Rev. Mater. Sci.* 1997; 27:1-34.
- [11] Terrones M. Science and Technology of the Twenty-First Century: Synthesis, Properties, and Applications of Carbon Nanotubes. *Annu. Rev. Mater. Res.* 2003; 33:419-501.
- [12] Oberlin A, Endo M, Koyama T. Filamentous Growth of Carbon Through Benzene Decomposition. *Journal of Crystal Growth* 1976; 32(3):335-349.
- [13] Iijima S. Helical Microtubules of Graphitic Carbon. *Nature* 1991; 354:56-58.
- [14] Iijima S, Ichihashi T. Single-Shell Carbon Nanotubes of 1-nm diameter. *Nature* 1993; 363(6430):603-605.

REFERENCES (continued)

- [15] Bethune DS, Klang CH, de Vries MS, Gorman G, Savoy R, Vazquez J, Beyers R. Cobalt-catalysed growth of carbon nanotubes with single-atomic-layer walls. *Nature* 1993; 363(6430):605-607.
- [16] Journet C, Maser WK, Bernier P, Loiseau A, Lamy de la Chapelle M, Lefrant S, Deniard P, Lee R, Fischer JE. Large-Scale Production of Single-Walled Carbon Nanotubes by the Electric-Arc Technique. *Nature* 1997; 388(6644):756-758.
- [17] T Guo, P Nikolaev, A Thess, DT Colbert, RE Smalley. Self-Assembly of Tubular Fullerenes. *J. Phys. Chem.* 1995; 99(27): 10694-1097.
- [18] A Thess, R Lee, P Nikolaev, H Dai, P Petit, J Robert, C Xu, YH Lee, SG Kim, AG Rinzler, DT Colbert, GE Scuseria, T Tomanek, JE Fischer, RE Smalley. Crystalline Ropes of Metallic Carbon Nanotubes. *Science* 1996; 273:483.
- [19] Eklund PC, Pradhan BK, Kim UJ, Xiong Q. Large-Scale Production of Single-Walled Carbon Nanotubes Using Ultrafast Pulses from a Free Electron Laser. *Nanoletters* 2002; 2(6):561-566.
- [20] Endo M, Takeuchi K, Igarashi S, Kobori K, Shiraishi M, Kroro H. The production and structure of Pyrolytic Carbon Nanotubes. *J. Phys. Chem. Solids* 1993; 54(12):1841-1848.
- [21] Meyyappan M, Delzeit L, Cassell A, Hash D. Carbon Nanotube Growth by PECVD: a review. *Plasma Sources Sci. Technol* 2003; 12:205-216.
- [22] Öncel Ç, Yürüm Y. Carbon Nanotube Synthesis via the Cathalytic CVD Method: A Review on the Effect of Reaction Parameters. *Fullerenes, Nanotubes, and Carbon Nanostructures* 2006; 14:17-37.
- [23] Hsu WK, Hare JP, Terrones M, Kroto HW, Walton DRM, Harris PJF. Condensed-phase nanotubes. *Nature* 1995; 377(6551):687.
- [24] Li WZ, Xie SS, Qian LX, Chang BH, Zou BS, Zhou WY, Zhao RA, Wang G. Large-Scale Synthesis of Aligned Carbon Nanotubes. *Science* 1996; 274:1701-1703.
- [25] Ren ZF, Huang ZP, Xu JW, Wang JH, Bush P, Siegal MP, Provencion PN. Synthesis of Large Arrays of Well-Aligned Carbon Nanotubes on Glass. *Science* 1998; 282:1105-1107.
- [26] Bower C, Zhu W, Sungho J, Zhou O. Plasma-induced alignment of carbon nanotubes. *Applied Physics Letters* 2000; 77(6):830-832.
- [27] Baker RTK. Catalytic Growth of Carbon Filaments. *Carbon* 1989; 27(3):315-323.

REFERENCES (continued)

- [28] Baird T, Fryer JR, Grant B. Carbon formation on iron and nickel foils by hydrocarbon pyrolysis-reactions at 700 °C. *Carbon* 1974; 12(5):591-602.
- [29] Lee CJ, Park J. Growth model of bamboo-shaped carbon nanotubes by thermal chemical vapor deposition. *Applied Physics Letters* 2000; 77(21):3397-3399.
- [30] Tibbetts G. Carbon Fibers Produced by Pyrolysis of Natural Gas in stainless steel tubes. *Applied Physics Letters* 1983; 42(8):666-668.
- [31] Bernholc J, Brenner D, Buongiorno Nardelli M, Meunier V, Roland C. Mechanical and electrical properties of nanotubes. *Annual Review of Materials Science* 2002; 32: 347-375.
- [32] Dresselhaus MS, Dresselhaus G, Jorio A. Unusual properties and structure of carbon nanotubes. *Annual Review of Materials Research* 2004; 34: 247-278.
- [33] Olk CH, Heremans JP. Scanning tunneling spectroscopy of carbon nanotubes. *Journal of Materials Research* 1994; 9(2): 259-262.
- [34] Weisman RB, Subramoney S. Carbon nanotubes. *Electrochemical Society Interface* 2006; 15(2): 42-46.
- [35] Treacy MMJ, Ebbesen TW, Gibson JM. Exceptionally high Young's modulus observed for individual carbon nanotubes. *Nature* 1996; 381(6584): 678.
- [36] Wang ZL, Gao RP, Poncharal P, de Heer WA, Dai ZR, Pan ZW. Mechanical and electrostatic properties of carbon nanotubes and nanowires. *Materials Science & Engineering C, Biomimetic and Supramolecular Systems* 2001; 16: 3-10.
- [37] Yu Min-Feng, Files BS, Arepalli S, Ruoff RS. Tensile loading of ropes of single wall carbon nanotubes and their mechanical properties. *Physical Review Letters* 2000; 84(24): 5552-5555.
- [38] Falvo MR, Clary GJ, Taylor RM II, Chi V, Brooks FP Jr, Washburn S, Superfine R. Bending and buckling of carbon nanotubes under large strain. *Nature* 1997; 389(6651): 582-584.
- [39] Iijima S, Brabec C, Maiti A, Bernholc J. Structural flexibility of carbon nanotubes. *Journal of Chemical Physics* 1996; 104(5): 2089.
- [40] Yi W, Lu L, Zhang D, Pan ZW, Xie SS. Linear specific heat of carbon nanotubes. *Physical Review B (Condensed Matter)* 1999; 59(14): 9015-9018.

REFERENCES (continued)

- [41] Kim P, Shi L, Majumdar A, McEuen PL. Thermal transport measurements of individual multiwalled nanotubes. *Physical Review Letters* 2001; 87(21): 215502/1-215502/4.
- [42] Maniwa Y, Fujiwara R, Kira H, Tou H, Kataura H, Suzuki S, Achiba Y, Nishibori E, Takata M, Sakata M, Fujiwara A, Suematsu H. Thermal expansion of single-walled carbon nanotube (SWNT) bundles: X-ray diffraction studies. *Physical Review B (Condensed Matter and Materials Physics)* 2001; 64(24): 241402/1-3.
- [43] Rueckes T, Kim K, Joselevich E, Tseng GY, Cheung CL, Lieber CM. Carbon nanotube-based nonvolatile random access memory for molecular computing. *Science* 2000; 289(5476): 94-97.
- [44] Baughman RH, Cui C, Zakhidov AA, Iqbal Z, Barisci JN, Spinks GM, Wallace GG, Mazzoldi A, De Rossi D, Rinzler AG, Jaszchinski O, Roth S, Kertesz M. Carbon nanotube actuators. *Science* 1999; 284(5418): 1340-1344.
- [45] Collins PG, Arnold MS, Avouris P. Engineering carbon nanotubes and nanotube circuits using electrical breakdown. *Science* 2001; 292(5517): 706-709.
- [46] Dai H, Hafner JH, Rinzler AG, Colbert DT, Smalley RE. Nanotubes as nanoprobe in scanning probe microscopy. *Nature* 1996; 384(6605): 147.
- [47] Wei XL, Chen Q, Liu Y, Peng LM. Cutting and Sharpening Carbon Nanotubes Using a Carbon Nanotube 'Nanoknife'. *Nanotechnology* 2007; 18: 185503/1-5.
- [48] Shigian Z, Oberdorster E, Haasch M. Toxicity of an engineered nanoparticle (fullerene, C₆₀) in two aquatic species, Daphnia and fathead minnow. *Marine Environmental Research* 2006; 62(Suppl. 1):S5-S9.
- [49] Yoko K, Yuka K, Atsuko M, Naoki M, Yoko Y. Fullerene as a novel photoinduced antibiotic. *Fullerenes Nanotubes and Carbon Nanostructures* 2003; 11(1):79-87.
- [50] Levi N, Hantgan R, Lively M, Carroll D, Gaddamanugu P. C₆₀-Fullerenes: Detection of intracellular photoluminescence and lack of cytotoxic effects. *Journal of Nanobiotechnology* 2006; 4:14.
- [51] Huczko A, Lange H, Calko E. Fullerenes: Experimental evidence for a null risk of skin irritation and allergy. *Fullerene Science and Technology* 1999; 7(5):935-939.
- [52] Huczko A, Lange H, Bystrzejewski M, Baranowski P, Grubek-Jaworska H, Nejman P, Przybylowski T, Czuminiska K, Glapinski J, Walton DRM, Kroto HW. Pulmonary Toxicity of 1-D nanocarbon materials.

REFERENCES (continued)

- [53] Muller J, Huaux F, Lison D. Respiratory Toxicity of Carbon Nanotubes: How worried should we be? *Carbon* 2006; 44:1048-1056.
- [54] Jia G, Wang H, Yan L, Wang X, Pei R, Yan T, Yuliang Z, Xinbiao G. Cytotoxicity of carbon nanomaterials: Single-wall nanotube, multi-wall nanotube, and fullerene. *Environmental Science and Engineering* 2005; 39(5):1378-1383.
- [55] Shvedova AA, Castranova V, Kisin ER, Schwegler-Berry D, Murray AR, Gandelsman VZ, Maynard A, Baron P. Exposure to carbon nanotube material: assessment of nanotube cytotoxicity using human keratinocyte cells. *J. Toxicol. Environ. Health.A* 2003; 66(20):1909-1926.
- [56] Warheit DB. What is currently known about the health risks related to carbon nanotube exposures? *Carbon* 2006; 44:1064-1069.
- [57] Huczko A, Lange H, Calko E, Grubek-Jaworska H, Droszcz P. Physiological Testing of Carbon Nanotubes: Are They Asbestos-Like? *Fullerene Science and Technology* 2001; 9(2):251-254.